Accepted Manuscript

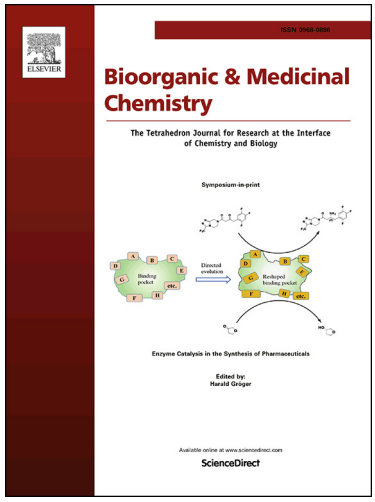

Synthesis and identification of 2,4-bisanilinopyrimidines bearing 2,2,6,6-tetramethylpiperidine-*N*-oxyl as potential Aurora A inhibitors

Chun-Yan Sang, Wen-Wen Qin, Xiu-Juan Zhang, Yu Xu, You-Zhen Ma, Xing-Rong Wang, Ling Hui, Shi-Wu Chen

PII: S0968-0896(18)31634-1
DOI: https://doi.org/10.1016/j.bmc.2018.11.006
Reference: BMC 14610

To appear in: *Bioorganic & Medicinal Chemistry*

Received Date: 19 September 2018
Revised Date: 16 October 2018
Accepted Date: 5 November 2018

Please cite this article as: Sang, C-Y., Qin, W-W., Zhang, X-J., Xu, Y., Ma, Y-Z., Wang, X-R., Hui, L., Chen, S-W., Synthesis and identification of 2,4-bisanilinopyrimidines bearing 2,2,6,6-tetramethylpiperidine-*N*-oxyl as potential Aurora A inhibitors, *Bioorganic & Medicinal Chemistry* (2018), doi: https://doi.org/10.1016/j.bmc.2018.11.006

Synthesis and identification of 2,4-bisanilinopyrimidines bearing 2,2,6,6-tetramethylpiperidine-*N*-oxyl as potential Aurora A inhibitors

Chun-Yan Sang [a], Wen-Wen Qin [a], Xiu-Juan Zhang [a], Yu Xu [a], You-Zhen Ma [a], Xing-Rong Wang [a], Ling Hui [b], Shi-Wu Chen [a,*]

[a] *School of Pharmacy, Lanzhou University, Lanzhou 730000, China*

[b] *Experimental Center of Medicine, General Hospital of Lanzhou Military Command, Lanzhou 730050, China*

* Corresponding author.

E-mail addresses: chenshw@lzu.edu.cn (S.-W. Chen)

Abstract: The Aurora kinases are a family of serine/threonine kinases that interact with components of the mitotic apparatus and serve as potential therapeutic targets in oncology. Herein, we reported a series of 2,4-bisanilinopyrimidines bearing 2,2,6,6-tetramethylpiperidine-*N*-oxyl with selective inhibition of Aurora A in either enzymatic assays or cellular phenotypic assays, and displaying more potent anti-proliferation compared with that of VX-680. The most potent compound **10a** forms better interaction with Aurora A than Aurora B in molecular docking. Mechanistic studies revealed that **10a** disrupt the spindle formation, block the cell cycle progression in the G2/M phase and induce apoptosis in HeLa cell. These results suggested that the produced series of compounds are potential anticancer agents for further development as selective Aurora A inhibitors.

Keywords: Aurora kinases; Stable nitroxides; Pyrimidine; Anticancer agents

1. Introduction

The Aurora kinase family is a subfamily of serine/threonine kinases that is essential for the regulation of centrosome maturation, mitotic spindle formation, chromosome segregation and cytokinesis during mitosis.[1,2] The family includes three kinases designated as Aurora A, B and C, which have sequences that are about 70% identity in the kinase domain. However, these kinases have quite different and nonoverlapping functions during mitosis.[3] Aurora A regulates the cell cycle and is associated with G2 phase and entry into the M phase, and associates with the spindle poles and is involved in both centrosomal and acentrosomal spindle assembly.[4,5] Aurora B has functions associates with histone phosphorylation and chromatin condensation in prophase, chromosome alignment and segregation, regulation of a mitotic checkpoint at metaphase and a role in cytokinesis.[6] Aurora C has similar functions as Aurora B, and plays important roles in regulating mitotic chromosome alignment, segregation and possibly cytokinesis. [7]

The role of Aurora kinase A and B in mitosis, coupled with evidence that amplification or over-expression of these kinases and other functions such as stabilization of *N*-myc by Aurora A drives tumorigenesis, has led to the development of numerous inhibitors that display selectivity to either Aurora A or Aurora B, or that are dual inhibitors.[8–10] Some of Aurora kinases inhibitors have been or are currently in clinical development, such as VX-680,[11,12] MLN8054,[13] ENMD-2076,[14] AMG 900,[15] CYC116[16] and PF-03814735[17,18] (Fig. 1).

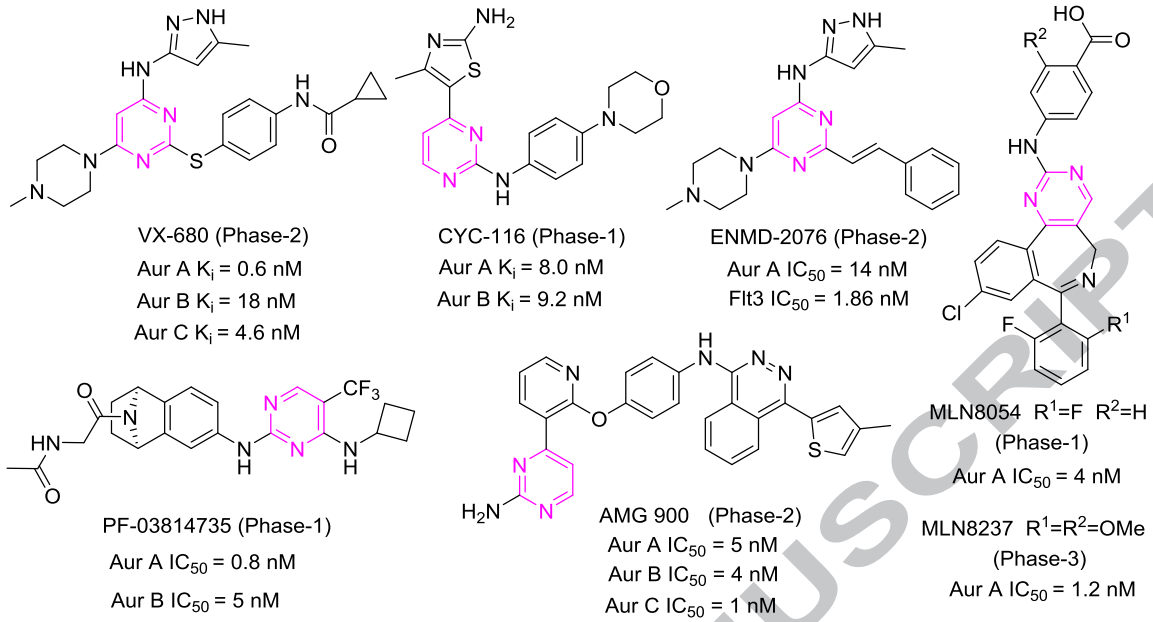

Fig. 1. Some representative Aurora kinases inhibitors.

Nitroxides are stable free radical species that possess a disubstituted nitrogen atom linked to a univalent oxygen atom and have a wide range of activities in biology.[19,20] Recently, with the development of cancer detection techniques, electron paramagnetic resonance (EPR) spin labeling using paramagnetic molecules, such as nitroxide free radicals, have gained considerable attention.[21] Previous studies have shown that the introduction of the nitroxyl moiety lead to a series of positive effects, such as higher alkylating, lower carbamoylating activity, better antimelanomic activity and lower general toxicity.[22] Recently, there are a number of studies that have successfully connected nitroxides and active molecules by appropriate linkers to find new antitumor agents.[23–25] We are also interested in nitroxide compounds, which have been found to be an available antitumor agents and their application has progressed significantly in the treatment of tumors.[26,27]

The bisanilinopyrimidine scaffold (such as compound **1**) has been reported

previously as a scaffold to develop inhibitors of Aurora kinases[28,29] and other kinases, such as JNK[30], FAK[31], EphB4[32,33], ALK[34,35], VEGFR[36], CDK2 and CDK4[37]. However, the generally lower potency of these compounds in cellular assays compared with that observed in enzymatic assays might reflect problems with the physical properties. We hypothesized that stable nitroxides labeled 2,4-bisanilinopyrimidines may be favorable Aurora kinase inhibitors with improved anticancer potency. Thus, we designed a series of 2,4-bisanilinopyrimidines bearing a nitroxyl group (Fig. 2), in which 4-amino-2,2,6,6-tetramethylpiperidine-*N*-oxyl (4-NH_2-TMPO) substituted the 4-acetylpiperazine at the pyrimidine 2-position of activity compound **1** in the literature.[29] Herein, we reported the synthesis of these compounds and identification of their antitumor effects as Aurora A kinase inhibitors.

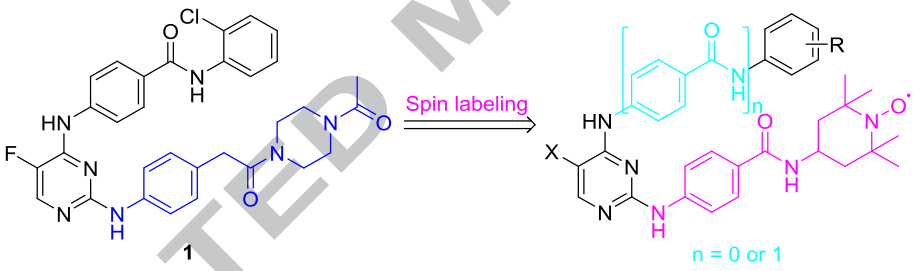

Fig. 2. Design of target compounds.

2. Results and discussion

2.1. Chemistry

Intermediates *p*-aminobenzamides **3a**−**e** were prepared by the protocols as illustrated in Scheme 1. Specifically, reaction of 4-((*tert*-butoxycarbonyl)amino)-benzoic acid with the appropriate amines (such as 4-NH_2-TMPO, *o*-, *m*-, *p*-chloride aniline, or *N*-methyl-4-amino-piperidine) in the presence of 1-(3-dimethylaminopropyl)-3-ethyl carbodiimide hydrochloride (EDCI), 1-hydroxybenzyltriazole hydrate (HOBt) in dry

dichloromethane (DCM) yielded the series of amides **2a–e**. Deprotection of **2a–e** with a solution of trifluoroacetic acid in dichloromethane generated the primary amines **3a–e**.[38]

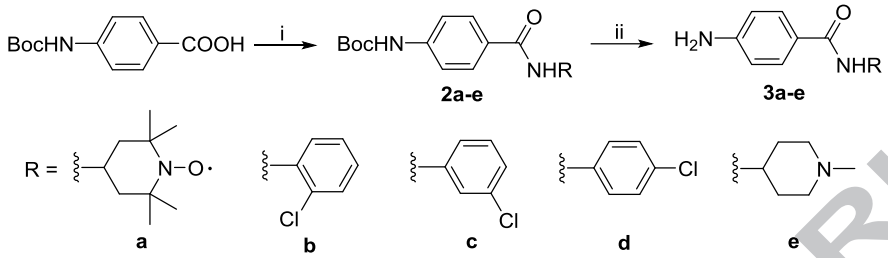

Scheme 1. Reagents and conditions: (i) EDCI, HOBt, DCM; (ii) 30% TFA in DCM.

Various libraries of 2,4-bisanilinopyrimidines bearing 2,2,6,6-tetramethylpiperidine-*N*-oxy were prepared in a straightforward way from corresponding 2,4-dichloropyrimidine (**4a−d**) as outlined in Scheme 2.[39,40] Briefly, the chlorine atoms at C4 and C2 of **4a−d** were sequentially displaced with the appropriate nucleophiles under different conditions to yield the desired target compounds **8–10**. For example, the intermediates **5a–c**, **6a–c** and **7a** were prepared by reaction of corresponding **4a–c** and appropriate amine (**3a**, or 2-chlorophenylamine, or **3b**) in the presence of *N*,*N*-diisopropylethylamine (DIPEA) in refluxing methanol with moderate yields. In contrast, the substitution of 2,4-dichloro-5-nitropyrimidine (**4d**) with appropriate amine (**3a–d**, or chlorophenylamine, or aminophenol) were easily completed in DCM at room temperature to provide intermediates **5d**, **6d–i** and **7b–d** in high yield. Subsequently, the chlorine atom at the 2-position of intermediates **5–7** was displaced with the appropriate nucleophiles (*p*-aminobenzoic acid for **8a–d**, **3a** for **9a–i** and **10a–d**) in refluxing 1,4-dioxoane under diluted HCl catalysis conditions to yield the corresponding target compounds **8–10**. In addition, reference compound **11**, which did not contain stable nitroxyl radicals, was also synthesized by treatment of **7a** with **3e** as synthetic procedure

for **10a**, as outlined in Scheme 3.

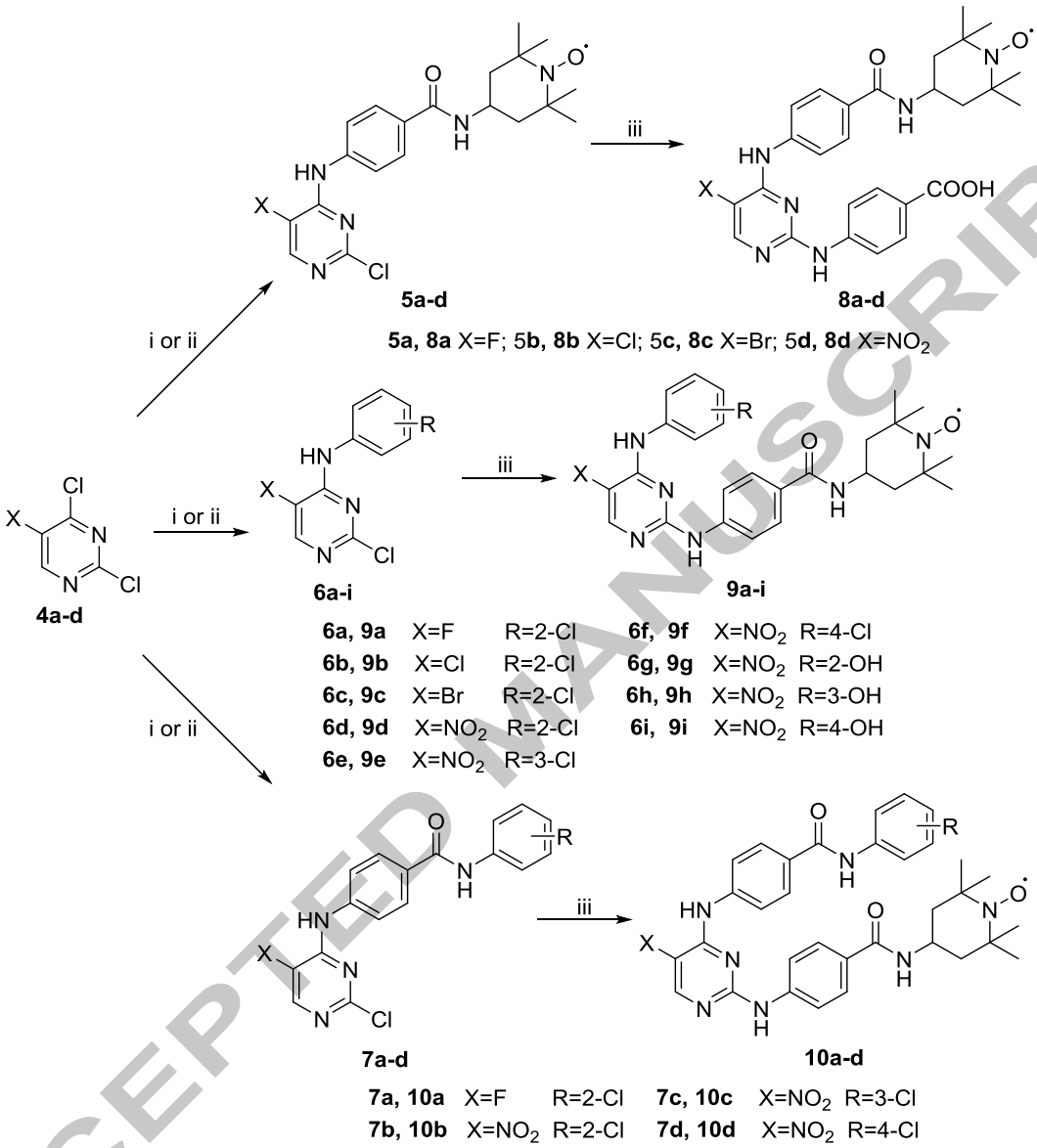

Scheme 2. Reagents and conditions: (i) **3a** (or 2-chlorophenylamine, or **3b**), DIPEA, MeOH, 70℃; (ii) **3a–d**, (or chlorophenylamine, or aminophenol), DCM, rt; (iii) *p*-aminobenzoic acid (or **3a**), refluxing 1,4-dioxoane, diluted HCl (4N HCl for **8a−c, 9a−c** and **10a**; 1N HCl for **8d, 9d−i** and **10b−d**).

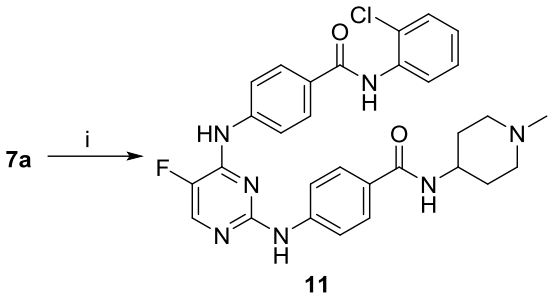

Scheme 3. Reagents and conditions: (i) **3e**, refluxing 1,4-dioxoane, 4N HCl.

The target synthetic compounds **8−11** were characterized by NMR, HRMS, ESR and IR based on the HPLC purity >95%. In NMR of free-radical labeled compounds **8−10**, some signals appear broadened and other signals are missing.[25]

2.2. Biological profiling

2.2.1. Anti-proliferative activities of compounds **8−11**

All the target compounds **8−11** were tested for anti-proliferative activities against four human tumor cell lines (cervical carcinoma HeLa, lung carcinoma A-549, hepatic carcinoma HepG2 and human colorectal adenocarcinoma LoVo cells) by MTT assays, with VX-680 as the reference compound.[38] The GI_{50} values of these compounds, which are the concentrations corresponding to 50% cells growth inhibition, are summarized in Tables 1.

Table 1 Anti-proliferative activities of target compounds **8−11** in human cancer cell lines

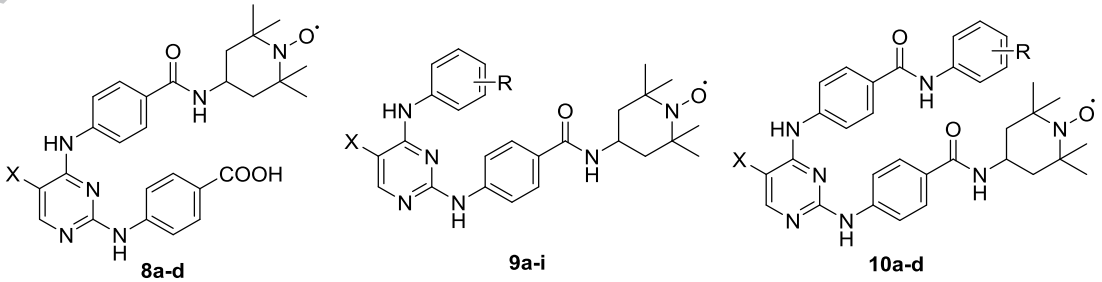

Compounds	X	R	Anti-proliferation (GI_{50}, μM)[a]			
			HeLa	A549	HepG2	LoVo
8a	F	--	21.3±2.3	18.5±2.1	26.8±3.5	65.3±5.0
8b	Cl	--	56.5±3.5	>100	48.2±4.5	56.6±4.0
8c	Br	--	>100	>100	35.8±2.5	>100
8d	NO_2	--	27.3±1.5	29.6±2.5	11.8±2.6	27.4±2.5
9a	F	2-Cl	8.4±1.2	2.3±0.5	1.2±0.5	2.7±2.0
9b	Cl	2-Cl	10.2±1.1	3.6±0.6	1.6±0.4	3.2±1.5
9c	Br	2-Cl	9.6±2.1	3.8±0.8	2.1±0.8	3.2±1.5
9d	NO_2	2-Cl	53.1±3.6	2.8±1.0	3.7±1.0	35.2±2.5
9e	NO_2	3-Cl	43.2±2.5	31.3±3.5	42.1±2.5	67.8±5.5
9f	NO_2	4-Cl	33.3±2.5	5.6±0.5	13.0±1.2	27.8±4.5
9g	NO_2	2-OH	13.9±1.5	11.2±0.8	3.7±1.3	28.3±3.5
9h	NO_2	3-OH	36.5±2.2	13.2±1.0	21.7±2.1	39.6±2.0
9i	NO_2	4-OH	34.3±1.8	14.3±1.5	21.5±3.5	43.8±3.0
10a	F	2-Cl	0.4±0.1	1.1±0.6	1.2±0.9	7.3±1.5
10b	NO_2	2-Cl	23.2±2.2	2.5±0.8	3.4±1.2	28.5±2.0
10c	NO_2	3-Cl	49.5±3.6	14.2±2.3	12.5±2.5	39.6±2.0
10d	NO_2	4-Cl	53.0±4.5	17.2±3.5	24.1±2.5	46.3±3.5
11	--	--	11.3±1.0	8.9±2.8	13.4±2.3	12.4±0.5
VX680	--	--	46.2±5.5	35.8±3.4	53.3±5.5	45.3±4.5

[a] Data are the mean of three independent experiments.

[b] drug exposure for 48 h.

Previous SAR studies have indicated that polar substituent at the *para* position of the benzene-ring at the pyrimidine 2-position is critical for potent anti-proliferative activity.[29] However, compounds **8a–d**, in which *p*-aminobenzamides of 4-NH_2-TMPO at the pyrimidine 4-position and polar substituent *p*-aminobenzoic acid at the pyrimidine

2-position, showed moderate even to weak anti-proliferation against these four cell lines. We speculated that the strong polarity of carboxyl group in these compounds resulted in their poor penetration and show weak anti-proliferative activity. So we adjusted the position of free radicals from 4-position to 2-position of pyrimidine as well as introduced the chlorophenylamine or aminophenol (which were the favorable groups to hold the anti-tumor activities of 2,4-bisanilinepymidines[29]) at the 4-position of pyrimidine to provide target compounds **9a**–**i**.

Inspiring, compounds **9a**−**d** showed stronger anti-proliferative activities against the four human tumor cell lines compared to VX-680. In particular, the GI_{50} values of **9a** for HeLa, A549, HepG2 and LoVo were 8.4±1.2, 2.3±0.5, 1.2±0.5 and 2.7±2.0 μM, respectively. The group (F, Cl, Br and NO_2) at the pyrimidine 5-position in these compounds (**9a**−**d**) gave no significant change to their proliferative inhibition. In the meantime, comparison of the GI_{50} values of compounds **9d**−**i** showed that hydroxy and chlorine in *ortho* position of the benzene ring gave more potent anti-proliferations than those of substitutions at the *meta* or *para* positions at the pyrimidine 4-position (**9d** *vs* **9e** and **9f**, **9g** *vs* **9h** and **9i**).

Then we extended the substitutes at 4-position of pyrimidines with the 4-amino-*N*-(chlorophenyl) benzamides (**3b–c**) to yield target compounds **10a–d**. We found that introduction of 4-amino-*N*-(chlorophenyl) benzamide at 4-position of pyrimidine slightly improved their anti-proliferation than those of chlorophenylamine (**10a** *vs* **6a**, **10b** *vs* **9d**, **10c** *vs* **9e**, **10d** *vs* **9f**). In addition, the *ortho*-chlorobenzene at 4-position of pyrimidine is critical for their ant-proliferation was obtained (**10b** *vs* **10c** and **10d**). Especially, compound **10a** showed the most potent anti-proliferative activity

in the series compounds against HeLa, A549, HepG2 and LoVo cells with GI_{50} values of 0.4±0.1, 1.1±0.6, 1.2±0.9 and 7.3±1.5 μM, respectively. Meanwhile, compound **10a** possesses more potent anti-proliferation than that of compound **11**, in which the 4-NH_2-TEMPO in **10a** was substituted with *N*-methyl-4-amino-piperidine. These results indicated that introduction of stable nitroxyl radical at the pyrimidine 2-position is favorable for generation of compounds that are retard cancer cell growth.

*2.2.2. Aurora kinases inhibition of compounds **9–11** in vitro*

Many pyrimidine compounds, such as VX-680, ENMD-2076, CYC-116 and PF-03814735, have entered clinical trials as Aurora kinases inhibitors.[10] Compounds **9–11**, which showed stronger anti-proliferative activities against the tested four human cancer cell lines, were tested for their Aurora kinases inhibitory activity using Kinase-Glo Plus luminescence kinase assay kit that measures ADP formation by Aurora kinases phosphorylation of the synthetic peptide LRRASLG, as described in the methods section, with VX-680 as the reference compound.[41]

As shown in Table 2, all the stable nitroxides labeled compounds **9a–i** and **10a–d** showed more excellent or comparable Aurora kinases inhibition in comparison to VX-680 and non-nitroxides labeled compound **11**. Moreover, most of this series compounds (except **9f**, **10b** and **10d**) exhibited selective inhibition of Aurora A over Aurora B. Especially, the most potent compound **10a**, with the IC_{50} values for Aurora A and Aurora B were 0.06 and 2.55 nM, respectively, showed 42-fold selectivity for Aurora A over Aurora B.

Aurora kinases inhibitory activities of compounds **9**–**10** showed various consistent with their anti-proliferation in different cell lines. For example, the Aurora A inhibitory

activities of compounds **9a-c** and **10a-d** were consistent with their anti-proliferation against HeLa and LoVo cells. In contrast, the Aurora B inhibitory activity of compounds **9d-f** was more consistent with anti-proliferative activity against A549 and HepG2 cells, which is in correlation with previous publication[42]. Considered compound **10a** showed the most potent inhibitory activities in either cell lines or Aurora kinases, following compound **10a** was selected to further study its action mechanism in HeLa cells.

Table 2. The Aurora kinases inhibitory activities of compounds **9–11** *in vitro*.

Compounds	(IC_{50}, nM)[a]		Compounds	(IC_{50}, nM)[a]	
	Aurora A	Aurora B		Aurora A	Aurora B
9a	0.18	1.11	**9i**	0.59	3.50
9b	0.19	0.29	**10a**	0.06	2.55
9c	0.46	2.67	**10b**	5.48	3.07
9d	1.86	3.29	**10c**	0.11	27.0
9e	0.62	19.5	**10d**	20.0	0.67
9f	1.61	0.34	**11**	2.28	49.1
9g	8.50	11.3	VX680	0.95	14.7
9h	0.14	3.50			

[a] The IC_{50} values are the means of two experiments.

*2.2.3. Compound **10a** selectively inhibits Aurora A over Aurora B in HeLa cells*

Aurora A kinase activity depends on autophosphorylation of Aurora A on Thr288 (p-Thr288) in the activation loop,[43] and Aurora B kinase activity bases on phosphorylation of Aurora B on Thr232 (p-Thr232).[44] Thus, evaluating the levels of p-Thr288 and p-Thr232 reflect the inhibitory activities of **10a** on the kinases in HeLa cells.

Firstly, HeLa cells were treated with various concentrations of compound **10a** (0, 1.25, 2.5, and 5.0 μM) for 12 h, and detected the expression of p-Thr288 and p-Thr232 in the cells by western blotting. As shown in Fig. 3A and Fig. 3B, compound **10a** induced the gradual decline of p-Thr288 and p-Thr232 HeLa cells in a dose dependent manner, and the degree of reduction of p-Thr288 was more than that of p-Thr232. These results revealed that **10a** possessed the selectivity for Aurora A over Aurora B. Furthermore, the inhibition effects of **10a** on either Aurora A or Aurora B were obviously higher than those of VX-680, which were consistent with their inhibition of Aurora kinases in vitro.

The selectivity of **10a** for Aurora A over Aurora B in HeLa cells were also confirmed by ELISA.[38] When HeLa cells were treated with less than 10 nM of compound **10a** for 12 h, the phosphorylation levels of Aurora A and B showed no significant changes. However, the concentration of **10a** was increased to more than 60 nM, the phosphorylation levels of Aurora A and B protein rapidly decreased, and the reduction of Aurora A was more than that of Aurora B in HeLa cell lysates. From Fig. 3C, we easily obtained the IC_{50} value of **10a** for Aurora A and B was 0.008 μM and 0.538 μM, respectively. However, the IC_{50} value of VX-680 for Aurora A and B was 0.013 μM and 0.148 μM, respectively (Fig. 3D). The data from the Aurora A and Aurora B cell-based assays suggest that **10a** has a 67-fold greater potency against Aurora A compared with Aurora B, and the selectivity of VX-680 for Aurora A over Aurora B was less than 12-fold.

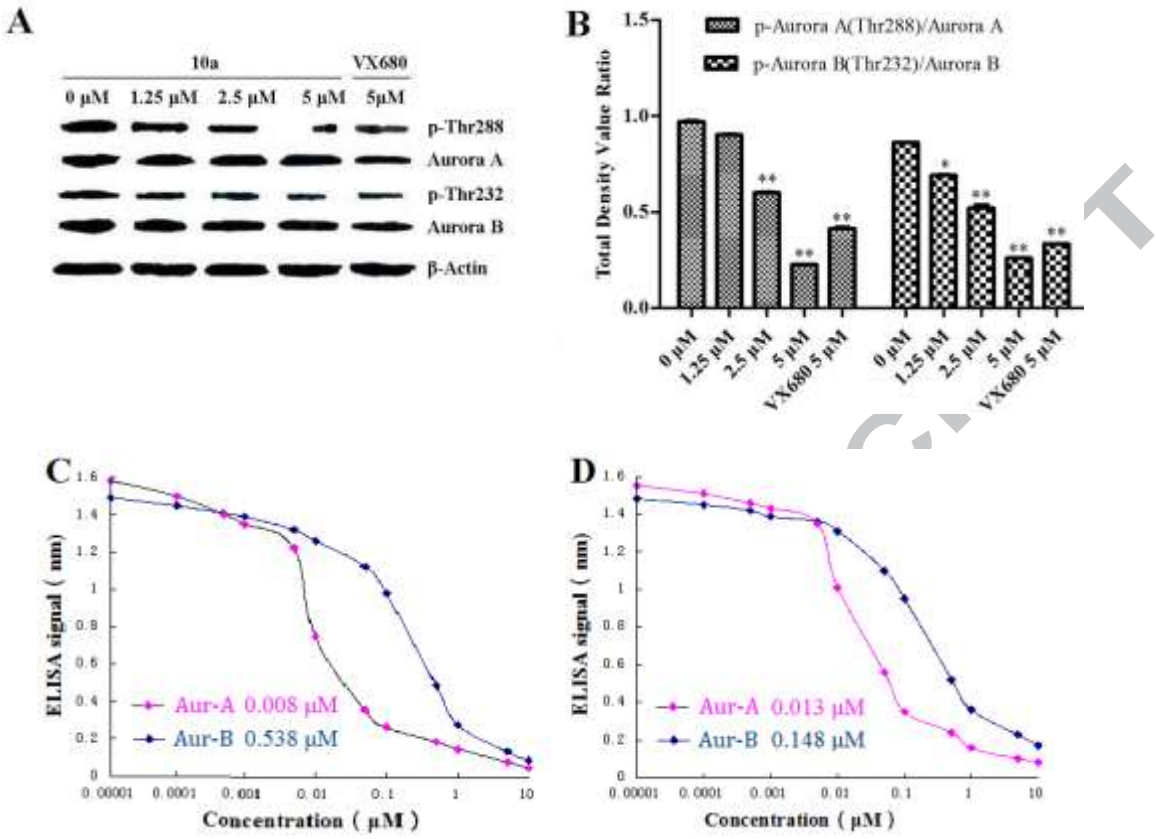

Fig. 3. Compound **10a** selectively inhibits Aurora A over Aurora B in HeLa cells. (A) Western blots of HeLa cells treated with various concentrations of **10a** probed for p-Thr288 and p-Thr232. (B) The results of western blots are expressed as the mean ± SD; **P* <0.05, ***P*<0.001 versus control. (C–D) ELISA analyzes of **10a** and VX-680 inhibits phosphorylation of Aurora A and Aurora B in HeLa cells.

*2.2.4. Compound **10a** disrupts spindle formation in HeLa cells*

Aurora A plays a pivotal role in centrosome maturation and spindle formation during mitosis, and over-expression of Aurora A provokes abnormalities in spindle formation, and the failure to complete spindle-microtubule attachment.[4,5] Thus, the morphology of mitotic spindles was examined in HeLa cells treated with **10a** at various concentrations and VX-680 for 24 h. As shown in Fig. 4, the DMSO treated control cells

displayed normal bipolar mitotic spindles. However, Compound **10a** at 0.1 μM or 1 μM induced the formation of abnormal mitotic spindles. Especially, when the concentration of compound **10a** was increased to 1 μM, the microtubule spindles wrapped around the cell nucleus have significantly shrunk and disorder formations. In contrast, VX680 treated cells still retained a spindle shaped microtubule network. These show that formation of abnormal mitotic spindles is consistent with a known Aurora A inhibition phenotype.[45]

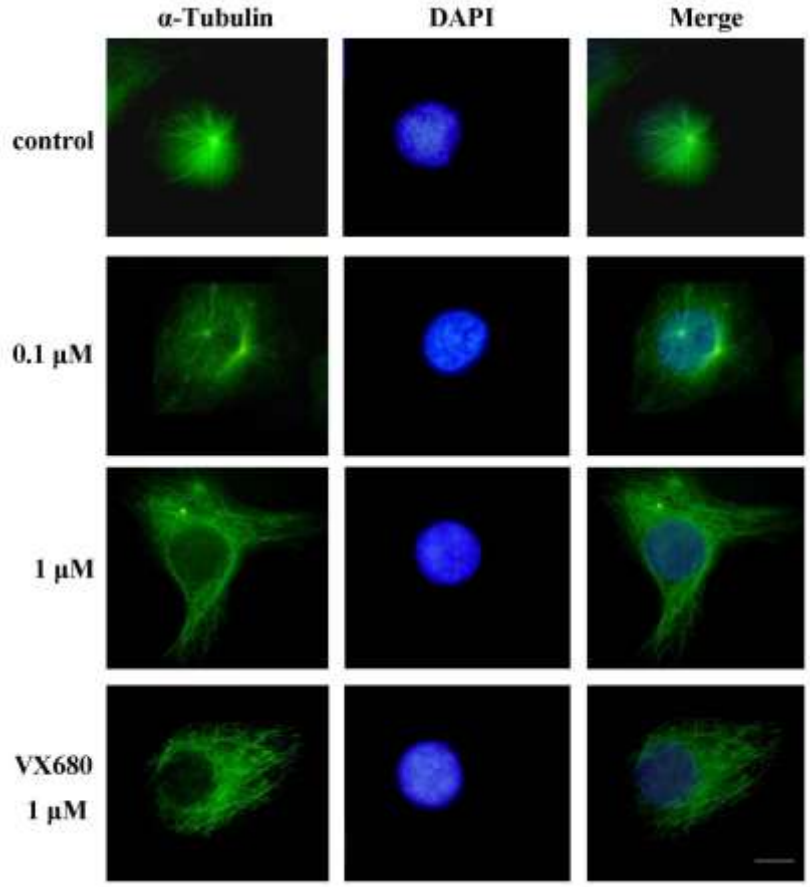

Fig. 4. Representative immunofluorescent images of HeLa cells treated with DMSO, **10a** (0.1 μM, or 1 μM), and VX680 (1 μM) for 24 h. Overlapped images were obtained from cells stained with anti-α-tubulin mouse antibody (tubulin; green) and DAPI (DNA; blue)

(Scale bars: 20 μm).

*2.2.5. Compound **10a** blocks the cell cycle in the G2/M phase in HeLa cells*

The Aurora inhibitors including VX-680 often induce common phenotypic effects of cancer cells such as cell cycle arrest at the G2/M phase. Thus, we also tested the effects of **10a** on cell cycle progression using fluorescence-activated cell sorting analysis of propidium iodide-stained in HeLa cells.[46] As shown in Fig. 5, treatment of HeLa cells with **10a** resulted in a dose-dependent accumulation of cells at the G2/M phase with a concomitant decrease in the population of G1 phase cells. Exposure to compound **10a** at 1 μM and 5 μM for 12 h, the percentages of cells at the G2/M phase arrest were 40.67% (Fig. 5B) and 60.33% (Fig. 5C), respectively, compared with 23.57% (Fig. 5A) in untreated cultures and 38.96% (Fig. 5D) in VX-680 treated cultures. Furthermore, cyclinB1 and cdc2 are two key regulators in the cell cycle progression,[47] to confirm the effects of **10a** in cell cycle arrest, we also measured their expression levels in HeLa cells after treatment with **10a** and VX-680. As shown in Fig. 5E and 5F, the levels of cyclinB1 and cdc2 protein marked decreased in HeLa cells with increasing treatment concentration of **10a** and VX-680 compared with that of control group. These results demonstrated that **10a** blocks the cell cycle in G2/M phase and displayed phenotypic characteristics similar to that of VX-680 in HeLa cells.

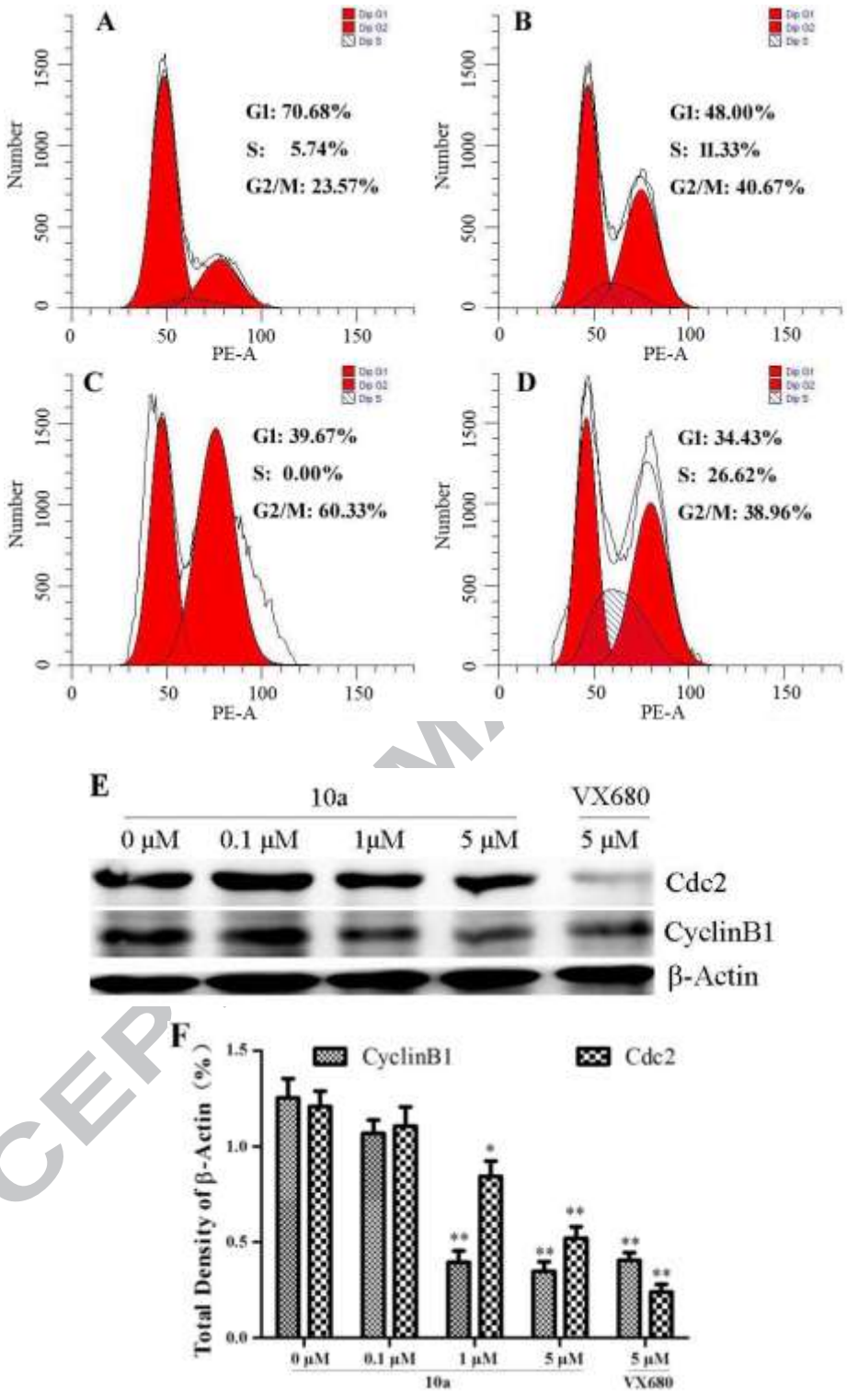

Fig. 5. Effects of **10a** on cell cycle progression. (A–D) HeLa cells were treated with DMSO, **10a** (1 μM, 5 μM), and VX680 (5 μM) for 12 h. Fixed and propidium iodide

(PI)-stained cells were analyzed by flow cytometry. (E) Western blot analysis of cyclinB1 and cdc2 in HeLa cells treated with **10a** or VX-680 for 12 h. (F) The results are expressed as the mean ± SD; **P* <0.05, ***P* <0.001 versus control.

*2.2.6. Compound **10a** induced apoptosis in HeLa Cell*

Previous publication[48] has revealed that inhibition of Aurora kinases not only inhibit proliferation but also induce apoptosis. To further certify whether **10a** induce apoptosis in HeLa cells, an annexin V-FITC/PI binding assay was performed. Specifically, HeLa cells were treated with **10a** at indicated concentrations, following the percentages of apoptotic cells were measured by flow cytometry. As shown in Fig. 6A–D, treatment of **10a** for 12 h gave substantial rise to the apoptotic ratios from 3.07% of vehicle control to 4.06% (0.1 μM), 11.34% (1 μM) and 28.9% (5 μM). These results demonstrated that **10a** exerted its anti-proliferative effects possibly by inducing apoptosis in HeLa cells.

Mitochondria represent the central checkpoint in propagating apoptotic signaling pathways, upon exposure to apoptotic stimuli, it can activate apoptosis-related proteins such as Bax, Bcl-2, and BAD to enter mitochondria, which induce the mitochondria to release cytochrome c and, in turn, activate the caspase-3 and -9, finally triggering the execution of apoptosis.[48] To explore the apoptotic mechanism of **10a** in HeLa cells, correspondent western blot analysis of apoptosis-related proteins were performed, and results were summarized in Fig. 6E–F. Treatment of **10a** for 12 h significantly up-regulated the expression of BAD, Bax, caspase-3, -9, together with down-regulation of Bcl-2. Thus, it was illuminated that **10a** induced cell apoptosis via the mitochondria-dependent pathway.

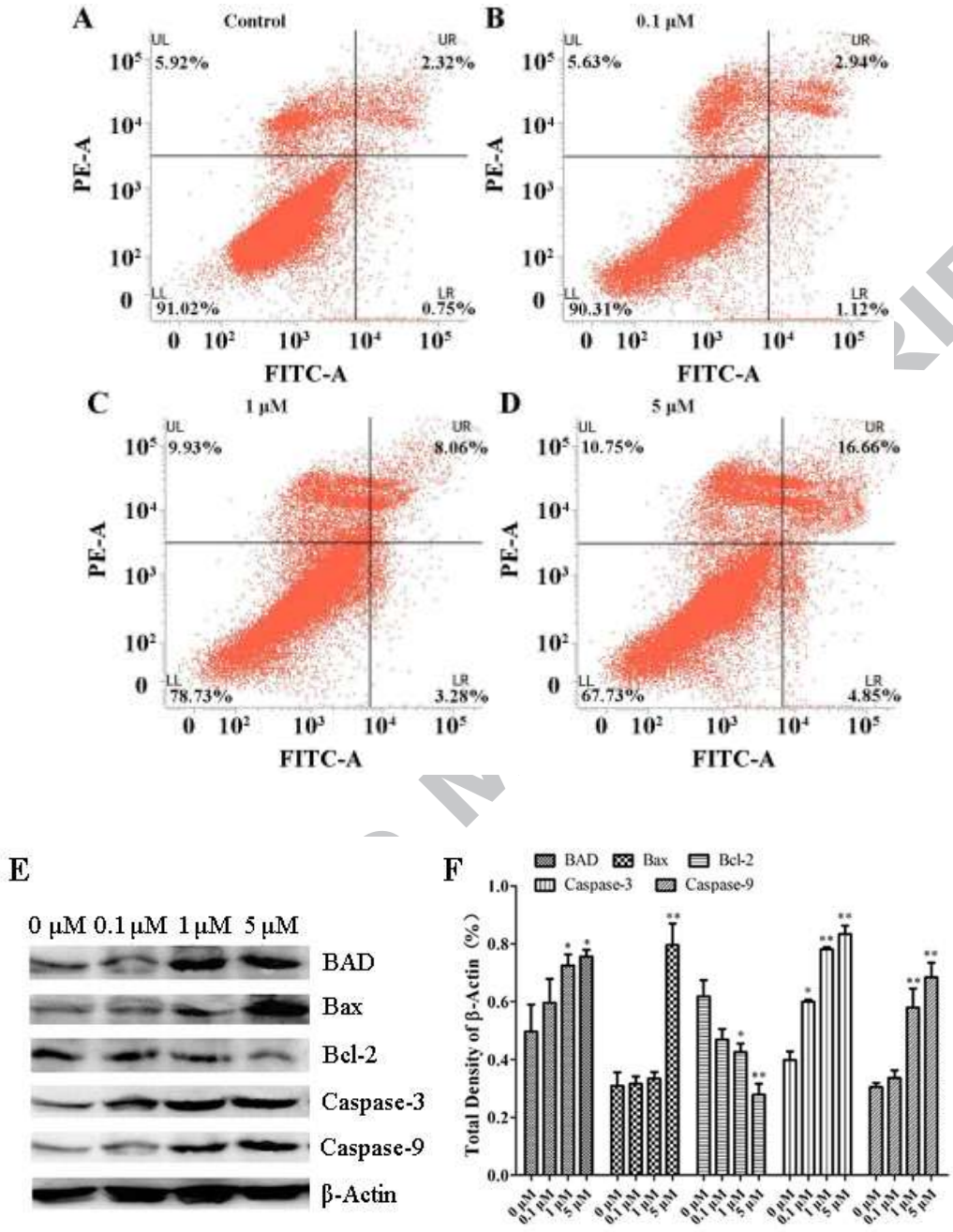

Fig. 6. Effects of **10a** induce apoptosis in the HeLa cells. (A–D) HeLa cells were treated with DMSO, **10a** (0.1 μM, 1 μM), and **10a** (5 μM) for 12 h, an annexin V-FITC/PI binding assay were performed by Annexin V-FITC apoptosis detection kit. (E) Western blot analysis of apoptosis-related proteins in HeLa cells treated with **10a** at 0.1 μM, 1 μM,

and 5 μM for 12 h. (F) The significantly expression change of the apoptotic proteins was analysed by immunoblotting (n=3; *$P<0.05$; #$P<0.01$).

*2.2.7. Binding model of compound **10a** with Aurora A*

To gain insight into the interaction of compound **10a** with Aurora A and Aurora B, docking simulation was performed using Schrödinger software (Maestro, version 10.1, Schrödinger, LLC, New York, NY, 2015).[49] All the figures displaying the docking results were obtained using the scientific software Pymol.[50] Grid was used to produce grids based on the position of the ligand in the proteins (PDB code 3E5A for Aurora A and 4AF3 for Aurora B). In the docking process, the protein was considered to be rigid, while the ligand was considered flexible. The ligand **10a** was docked into the appropriate binding pocket of Aurora A and Aurora B using the dock module and the calculated binding energy was –44.40 kcal/mol for Aurora A and –31.01 kcal/mol for Aurora B, respectively. The resulting docking poses are shown in Figure 7. According to the binding energy, **10a** is more sensitive to Aurora A than Aurora B.

Overall, the binding pockets of Aurora A and Aurora B are highly hydrophobic. Thus, hydrophobic interactions are the main driving force for the binding of **10a** to Aurora A and Aurora B. In Aurora A, **10a** can form several H-bonds, such as the nitrogen atom of N-1 in pyrimidine with hinge region Ala213, the oxygen atom of carbonyl group in C-2 of pyrimidine with hinge region Try212, and the oxygen atom of nitroxide with Lys162. Simultaneously the hydrophilic region is very well occupied by nitroxide in **10a** (Fig. 7A). However, in Aurora B, **10a** only can form one H-bonds of the oxygen atom of carbonyl group connected to *p*-chloride aniline with Pro158 (Fig. 7C). Additionally, from the shape of the binding pocket, **10a** can fit much better with the binding pocket of

Aurora A than Aurora B (Fig. 7B and 7D). These differences may explain why compound **10a** binds better with Aurora A compared with Aurora B.

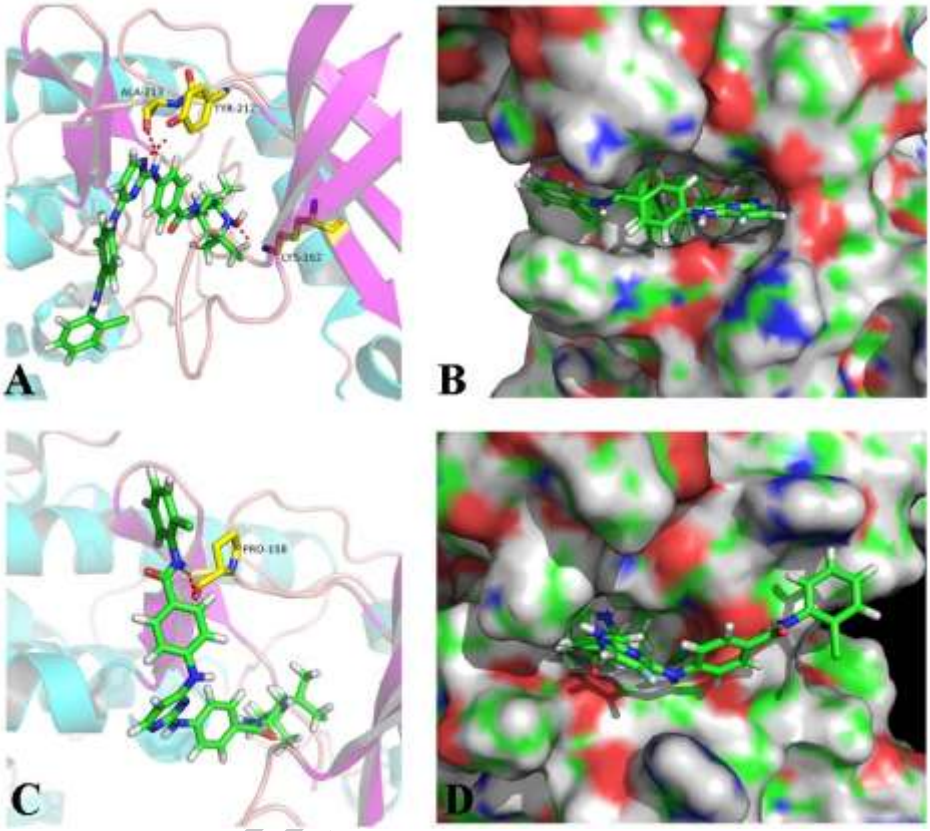

Fig. 7. Binding modes of **10a** with Aurora A and Aurora B. The dashed lines indicate hydrogen bonding interactions between the ligand and the protein. (A) The interaction between **10a** and Aurora A (PDB ID: 3E5A). (B) The binding pocket of Aurora A was shown in surface. (C) The interaction between **10a** and Aurora B (PDB ID: 4AF3). (D) The binding pocket of Aurora B was shown in surface.

3. Conclusion

In summary, Aurora kinases have been of interest as potential therapeutic targets in oncology. In this work, a series of stable nitroxyl radicals labeled 2,4-bisanilinopyrimidines as small molecule Aurora kinases inhibitors exert potent

anticancer activities. We specifically demonstrated that compound **10a** was selective inhibition of Aurora A over Aurora B either in vitro or in HeLa cells, arrested cell cycle in the G2/M phase, and induced cell apopotosis. The present investigation indicates that compound **10a** possesses potent antitumor activity as an Aurora A inhibitor for further development.

4. Experimental protocols

4.1. Chemistry

General. Melting points were determined with a XT_4-100 apparatus and are uncorrected. ^{1}H NMR and ^{13}C NMR spectra were recorded using a Agilent NMR inova600 spectrometer. EPR spectra were recorded with a Bruker A300 X-band EPR spectrometer. Mass spectra were recorded on a Bruker Dalton APEXII 49e, micrOTOF and Esquire6000 spectrometer with ESI source as ionization, respectively. IR spectra were obtained with a Nicolet iS5-IR spectrometer on neat samples placed between KBr plates. The purities of all of the biologically tested compounds were estimated by HPLC, and in each case, the major peak accounted for ≥95% of the combined total peak area when monitored by a UV detector. HPLC analysis using a UltiMate300 DAD HPLC system equipped with a PU-2089 Plus quaternary gradient pump and a UV-2075 Plus UV−vis detector, using an Alltech Kromasil C18 column with dimensions of 250 mm×4.6 mm and 5 μm particle size. Analytical thin-layer chromatography was conducted on silica gel GF_{254} plates (0.25 mm thick), and compounds were visualized with UV light at 254 nm. Silica gel flash chromatography was performed using Silica Gel 60 (200–300 mesh, Qingdao Ocean Chemical Ltd., China).

*4.1.1. General procedures for preparation of 4-Aminobenzenamides **3a–e***

To a solution of 4-((*tert*-butoxycarbonyl)amino)-benzoic acid (1.8 g, 7.2 mmol) in dry CH_2Cl_2 (20 mL) were added EDCI (1.8 g, 9 mmol), HOBt (1.22 g, 9 mmol). After stirring at room temperature for 1 h, 4-NH_2-TEMPO (or 2-, 3-, 4-chloroaniline, or *N*-methyl-4-amino-piperidine) (9 mmol) was added and the reaction continued for another 24 h at room temperature under argon. Water (200 mL) was then added and the mixture stirred for 5 min. The product was then extracted with ethyl acetate (3×30 mL). The combined organic extracts were washed with brine (30 mL), dried over sodium sulfate, filtered, and the solvent removed. Purification was achieved by flash chromatography (dichloromethane/acetone 20:1 by volume) to yield pure **2a**−**e**.

*4.1.1.1. tert-Butyl (4-((2,2,6,6-tetramethyl-1-oxyl)carbamoyl)phenyl)carbamate (**2a**)* Yield: 90%; Pink solid; ^{1}H NMR (600 MHz, DMSO-d_6) (*note compound is a free-radical, some signals appear broadened and other signals are missing) δ 9.63 (s, 1 H), 7.78 (s, 2 H), 7.53 (s, 2 H), 1.47 (s, 9 H).

*4.1.1.2. tert-Butyl (4-((2-chlorophenyl)carbamoyl)phenyl)carbamate (**2b**)* Yield: 62%; White solid; ^{1}H NMR (600 MHz, $CDCl_3$) δ 8.20 (d, *J* = 8.4 Hz, 2 H), 8.10 (d, *J* = 8.4 Hz, 1 H), 7.61 (d, *J* = 8.4 Hz, 2 H), 7.55 (t, *J* = 8.4 Hz, 1 H), 7.48 (d, *J* = 7.8 Hz, 1 H), 7.45 (t, *J* = 7.8 Hz, 1 H), 6.97 (s, 1 H), 6.94 (s, 1 H), 1.55 (s, 9 H).

*4.1.1.3. tert-butyl (4-((3-chlorophenyl)carbamoyl)phenyl)carbamate (**2c**)* Yield: 64%; White solid; ^{1}H NMR (600 MHz, DMSO-d_6) δ 10.25 (s, 1 H), 9.75 (s, 1 H), 7.97 (s, 1 H), 7.90 (d, *J* = 9.0 Hz, 2 H), 7.70 (d, *J* = 7.8 Hz, 1 H), 7.60 (d, *J* = 8.4 Hz, 2 H), 7.37 (t, *J* = 8.4 Hz, 1 H), 7.14 (d, *J* = 7.8 Hz, 1 H), 1.49 (s, 9 H).

*4.1.1.4. tert-butyl (4-((4-chlorophenyl)carbamoyl)phenyl)carbamate (**2d**)* Yield: 59%; White solid; ^{1}H NMR (600 MHz, DMSO-d_6) δ 10.02 (brs, 1 H), 9.32 (s, 1 H), 7.88 (d, *J* = 8.4 Hz, 2 H), 7.80 (d, *J* = 9.0 Hz, 2 H), 7.60 (d, *J* = 8.4 Hz, 2 H), 7.27 (d, *J* = 8.4 Hz, 1 H), 1.49 (s, 9 H).

*4.1.1.5. tert-Butyl (4-((1-methylpiperidin-4-yl)carbamoyl)phenyl)carbamate (**2e**)* Yield: 53%; White solid; ^{1}H NMR (600 MHz, DMSO-d_6) δ 9.58 (s, 1 H), 8.16 (d, *J* = 7.8 Hz, 1 H), 7.77 (d, *J* = 8.4 Hz, 2 H), 7.50 (d, *J* = 8.4 Hz, 2 H), 3.84–3.80 (m, 1 H), 2.99–2.96 (m, 2 H), 2.45–2.34 (m, 5 H), 1.83–1.79 (m, 2 H), 1,70–1.67 (m, 2 H), 1.47 (s, 9 H).

A solution of **2a−e** (5 mmol) in 30% dichloromethane solution of trifluoroacetic acid (20 mL) was stirred at room temperature for 1 h. The solvent was evaporated in vacuo, and diethyl ether (15 mL) was added. The precipitate was collected, washed with ether and dried to provide white solid **3a−e** and be used in the next reaction without further purification.

*4.1.2. General procedure for the synthesis of intermediates **5a−d**, **6a−i**, **7a−d***

Method 1: To a solution of 2,4-dichloro-5-fluoropyrimidine (**4a**, 0.23 g, 1.4 mmol) in MeOH (10 mL) at room temperature was added **3a** (0.35 g, 1.2 mmol) and DIPEA (0.2 mL, 1.2 mmol). The resulting mixture was refluxed for another 12 h (monitored by TLC). After cooling to room temperature, the precipitate **5a** was filtrated and washed with MeOH. Similar synthetic procedures were operated to give pure **5b−c**, **6a−c** and **7d**.

Method 2: To a solution of 2,4-dichloro-5-nitropyrimidine (**4d**, 0.27 g, 1.4 mmol) in DCM (20 mL) at rt was added **3a** (0.35 g, 1.2 mmol), and stirred for another 12 h (monitored by TLC). The precipitate **5d** was filtrated and washed with DCM. Similar procedures were operated to provide pure **6d−i** and **7a−c**.

*4.1.2.1. 4-((2-Chloro-5-fluoropyrimidin-4-yl)amino)-N-(2,2,6,6-tetramethyl-1-oxyl) benzamide (**5a**).* Yield: 67%; White solid; ^{1}H NMR (600 MHz, DMSO-d_6) (*note compound is a free-radical, some signals appear broadened and other signals are missing) δ 9.63 (s, 1 H), 7.78 (s, 2 H), 7.53 (s, 2 H); MS (ESI) *m/z*: 422.4 ([M+2]$^+$, 100%).

*4.1.2.2. 4-((2,5-Dichloropyrimidin-4-yl)amino)-N-(2,2,6,6-tetramethyl-1-oxyl) benzamide (**5b**).* Yield: 55%; White solid; ^{1}H NMR (600 MHz, DMSO-d_6) (*note compound is a free-radical, some signals appear broadened and other signals are missing) δ 9.63 (s, 1 H), 7.78 (s, 2 H), 7.53 (s, 2 H); MS (ESI) *m/z*: 440.1 ([M+4]$^+$, 100%); 438.1 ([M+2]$^+$, 85%).

*4.1.2.3. 4-((5-Bromo-2-chloropyrimidin-4-yl)amino)-N-(2,2,6,6-tetramethyl-1-oxyl) benzamide (**5c**).* Yield: 58%; White solid; ^{1}H NMR (600 MHz, DMSO-d_6) (*note compound is a free-radical, some signals appear broadened and other signals are missing) δ 9.63 (s, 1 H), 7.78 (s, 2 H), 7.53 (s, 2 H); MS (ESI) *m/z*: 484.2 ([M+4]$^+$, 100%), 482.2 ([M+2]$^+$, 84%).

*4.1.2.4. 4-((2-Chloro-5-nitropyrimidin-4-yl)amino)-N-(2,2,6,6-tetramethyl-1-oxyl) benzamide (**5d**).* Yield: 63%; Yellow solid; ^{1}H NMR (600 MHz, DMSO-d_6) (*note compound is a free-radical, some signals appear broadened and other signals are missing) δ 9.63 (s, 1H), 7.78 (s, 2H), 7.53 (s, 2H); MS (ESI) *m/z*: 449.5 ([M+2]$^+$, 100%).

*4.1.2.5. 2-Chloro-N-(2-chlorophenyl)-5-fluoropyrimidin-4-amine (**6a**).* Yield: 76%; White solid; ^{1}H NMR (600 MHz, $CDCl_3$) δ 8.51 (d, *J* = 8.4 Hz, 1 H), 8.13 (d, *J* = 2.4 Hz, 1 H), 7.56 (s, 1 H), 7.44 (d, *J* = 8.4 Hz, 1 H), 7.37 (t, *J* = 7.2 Hz, 1 H), 7.11 (t, *J* = 7.2 Hz, 1 H).

*4.1.2.6. 2,5-Dichloro-N-(2-chlorophenyl)pyrimidin-4-amine (**6b**).* Yield: 69%; White solid; ^{1}H NMR (600 MHz, $CDCl_3$) δ 8.52 (d, *J* = 8.4 Hz, 1 H), 8.26 (s, 1 H), 7.97 (brs, 1 H), 7.44 (d, *J* = 7.8 Hz, 1 H), 7.37 (t, *J* = 7.2 Hz, 1 H), 7.11 (t, *J* = 7.2 Hz, 1 H).

*4.1.2.7. 5-Bromo-2-chloro-N-(2-chlorophenyl)pyrimidin-4-amine (**6c**)* Yield: 75%; White solid; ^{1}H NMR (600 MHz, $CDCl_3$) δ 8.51 (d, *J* = 7.8 Hz, 1 H), 8.36 (s, 1 H), 8.01 (brs, 1 H), 7.44 (d, *J* = 8.4 Hz, 1 H), 7.37 (t, *J* = 7.8 Hz, 1 H), 7.11 (t, *J* = 7.8 Hz, 1 H).

*4.1.2.8. 2-Chloro-N-(2-chlorophenyl)-5-nitropyrimidin-4-amine (**6d**)*. Yield: 89%; Yellow solid; ^{1}H NMR (600 MHz, $CDCl_3$) δ 10.68 (brs, 1 H), 9.22 (s, 1 H), 8.33 (d, *J* = 7.8 Hz, 1 H), 7.50 (d, *J* = 7.8 Hz, 1 H), 7.39 (t, *J* = 7.8 Hz, 1 H), 7.23 (t, *J* = 7.8 Hz, 1 H).

*4.1.2.9. 2-Chloro-N-(3-chlorophenyl)-5-nitropyrimidin-4-amine (**6e**)*. Yield: 68%; Yellow solid; ^{1}H NMR (600 MHz, DMSO-d_6) δ 10.52 (s, 1 H), 9.19 (s, 1 H), 7.68 (s, 1 H), 7.53 (d, *J* = 8.4 Hz, 1 H), 7.47 (t, *J* = 8.4 Hz, 1 H), 7.36 (d, *J* = 8.4 Hz, 1 H).

*4.1.2.10. 2-Chloro-N-(4-chlorophenyl)-5-nitropyrimidin-4-amine (**6f**)*. Yield: 82%; Yellow solid; ^{1}H NMR (600 MHz, DMSO-d_6) δ 10.51 (s, 1 H), 9.17 (s, 1 H), 7.56 (d, *J* = 8.4 Hz, 2 H), 7.51 (d, *J* = 9.0 Hz, 2 H).

*4.1.2.11. 2-((2-Chloro-5-nitropyrimidin-4-yl)amino)phenol (**6g**)*. Yield: 76%; Red solid; ^{1}H NMR (600 MHz, DMSO-d_6) δ 9.43 (brs, 1 H), 9.05 (s, 1 H), 8.83 (s, 1 H), 8.59 (d, *J* = 8.4 Hz, 1 H), 7.09 (t, *J* = 7.8 Hz, 1 H), 6.94 (d, *J* = 8.4 Hz, 1 H), 6.86 (t, *J* = 7.8 Hz, 1 H); MS (ESI) 265.3 ([M–1]$^-$).

*4.1.2.12. 3-((2-Chloro-5-nitropyrimidin-4-yl)amino)phenol (**6h**)*. Yield: 86%; Yellow solid; ^{1}H NMR (600 MHz, DMSO-d_6) δ 10.60 (s, 1 H), 8.97 (s, 1 H), 8.47 (d, *J* = 7.8 Hz, 1 H), 6.98 (s, 2 H), 6.83 (t, *J* = 8.4 Hz, 1 H); MS (ESI) 265.5 ([M–1]$^-$).

*4.1.2.13. 4-((2-Chloro-5-nitropyrimidin-4-yl)amino)phenol (**6i**)*. Yield: 74%; Red solid; ^{1}H NMR (600 MHz, DMSO-d_6) δ 10.29 (s, 1 H), 9.58 (brs, 1 H), 9.10 (s, 1 H), 7.28 (d, *J* = 9.0 Hz, 2 H), 6.81 (d, *J* = 9.0 Hz, 2 H); MS (ESI) 265.6 ([M–1]$^-$).

*4.1.2.14. 4-((2-Chloro-5-fluoropyrimidin-4-yl)amino)-N-(2-chlorophenyl)benzamide (**7a**)*.

Yield: 54%; White solid; ^{1}H NMR (600 MHz, DMSO-d_6) δ 10.26 (s, 1 H), 9.95 (s, 1 H), 8.41 (d, *J* = 3.6 Hz, 1 H), 8.02 (d, *J* = 7.2 Hz, 2 H), 7.88 (d, *J* = 7.2 Hz, 2 H), 7.63 (d, *J* = 7.8 Hz, 1 H), 7.56 (d, *J* = 8.4 Hz, 1 H), 7.39 (t, *J* = 7.8 Hz, 1 H), 7.29 (t, *J* = 7.8 Hz, 1 H).

*4.1.2.15. 4-((2-Chloro-5-nitropyrimidin-4-yl)amino)-N-(2-chlorophenyl)benzamide (**7b**).* Yield: 49%; Yellow solid; ^{1}H NMR (600 MHz, DMSO-d_6) δ 10.59 (s, 1 H), 10.10 (s, 1 H), 9.19 (s, 1 H), 8.04 (d, *J* = 8.4 Hz, 2 H), 7.72 (d, *J* = 9.0 Hz, 2 H), 7.59 (d, *J* = 8.4 Hz, 1 H), 7.56 (d, *J* = 8.4 Hz, 1 H), 7.39 (t, *J* = 7.8 Hz, 1 H), 7.30 (t, *J* = 7.8 Hz, 1 H).

*4.1.2.16. 4-((2-Chloro-5-nitropyrimidin-4-yl)amino)-N-(3-chlorophenyl)benzamide (**7c**).* Yield: 79%; Yellow solid; ^{1}H NMR (600 MHz, DMSO-d_6) δ 10.61 (s, 1 H), 10.47 (s, 1 H), 9.21 (s, 1 H), 8.03–7.99 (m, 3 H), 7.75–7.71 (m, 3 H), 7.39 (t, *J* = 7.8 Hz, 1 H), 7.30 (d, *J* = 7.8 Hz, 1 H).

*4.1.2.17. 4-((2-Chloro-5-nitropyrimidin-4-yl)amino)-N-(4-chlorophenyl)benzamide (**7d**).* Yield: 86%; Yellow solid; ^{1}H NMR (600 MHz, DMSO-d_6) δ 10.58 (s, 1 H), 10.41 (s, 1 H), 9.19 (s, 1 H), 8.00 (d, *J* = 8.4 Hz, 2 H), 7.82 (d, *J* = 9.0 Hz, 2 H), 7.72 (d, *J* = 8.4 Hz, 2 H), 7.41 (d, *J* = 9.0 Hz, 2 H).

4.1.3. *General synthetic procedures for compounds **8-11***

Intermediate **5a** (210 mg, 0.5 mmol) and *p*-aminobenzoic acid (137 mg, 1 mmol) were dissolved in 25 mL 1,4-dioxoane, following 4N HCl (0.4 mL) was added, and the mixture was refluxed for 24 h. After cooling to room temperature, the precipitate was filtrated and washed with DCM. The precipitate was further purified by column chromatography on silica gel gave desired product **8a**. Similar procedures were operated to provide pure **8b–d**, **9a–i**, **10a–d** and **11**.

4.1.3.1. 4-((5-Fluoro-4-((4-((2,2,6,6-tetramethyl-1-oxyl)carbamoyl)phenyl)amino)

*pyrimidin-2-yl)amino)benzoic acid (**8a**)*. Yield: 39%; White solid; m.p.: 226–228℃; IR (KBr, cm^{-1}) 3334, 3194, 2965, 1721, 1614, 1526, 1424, 1387, 1327, 1202, 1172, 843, 763; ^{1}H NMR (600 MHz, DMSO-d_6) (*note compound is a free-radical, some signals appear broadened and other signals are missing) δ 9.65 (s, 1H), 9.60 (s, 1H), 8.22 (s, 1H), 7.96 (s, 2H), 7.79 (s, 2H); ^{13}C NMR (150 MHz, DMSO-d_6) δ 164.7, 154.4, 148.7, 142.9, 141.0, 140.7, 139.5, 130.7, 128.6, 127.3, 119.5, 116.8. ESR (DMSO): g = 2.006, An (G) = 15.94, ΔH (G) = 2.64. LC-MS (ESI) *m/z* (rel intensity) 523.2 ($[M+2H]^+$, 100); HRMS (ESI) 523.2457 for $[M+2H]^+$ (calcd 523.2464 for $C_{27}H_{32}N_6O_4F$). HPLC purity 97.1% (MeOH: H_2O (0.1%TFA) = 60:40, 0.8 mL/min, t_R = 10.03 min).

*4.1.3.2. 4-((5-Chloro-4-((4-((2,2,6,6-tetramethyl-1-oxyl)carbamoyl)phenyl)amino) pyrimidin-2-yl)amino)benzoic acid (**8b**)* Yield: 57%; White solid; m.p.: 245–247℃; IR (KBr, cm^{-1}) 3334, 3189, 2945, 1718, 1659, 1616, 1579, 1531, 1501, 1447, 1424, 1329, 1200, 1170, 1085, 843, 766; ^{1}H NMR (600 MHz, DMSO-d_6) (*note compound is a free-radical, some signals appear broadened and other signals are missing) δ 9.68 (s, 1H), 9.09 (s, 1H), 8.24 (s, 1H), 7.86 (s, 5H), 7.75 (s, 3H); ^{13}C NMR (150 MHz, DMSO-d_6) δ 164.3, 156.1, 154.5, 141.8, 140.2, 126.8, 126.7, 121.0, 116.8, 104.0; ESR (DMSO): g = 2.006, An (G) = 15.96, ΔH (G) = 3.15. LC-MS (ESI) *m/z* (rel intensity) 539.2 ($[M+2H]^+$, 100); HRMS (ESI) 539.2162 for $[M+2H]^+$ (calcd 539.2168 for $C_{27}H_{32}N_6O_4Cl$). HPLC purity 97.6% (MeOH: H_2O (0.1%TFA) = 50:50, 0.8 mL/min, t_R = 12.44 min).

*4.1.3.3. 4-((5-Bromo-4-((4-((2,2,6,6-tetramethyl-1-oxyl)carbamoyl)phenyl)amino) pyrimidin-2-yl)amino)benzoic acid (**8c**)* Yield: 50%; White solid; m.p.: 267–269℃; IR (KBr, cm^{-1}) 3336, 3189, 2990, 1718, 1656, 1616, 1569, 1526, 1422, 1327, 1207, 1172, 843, 763; ^{1}H NMR (600 MHz, DMSO-d_6) (*note compound is a free-radical, some

signals appear broadened and other signals are missing) δ 9.67 (s, 1H), 8.84 (s, 1H), 8.32 (s, 1H), 7.92 (s, 1H), 7.80 (s, 2H), 7.71 (s, 5H); ^{13}C NMR (150MHz, DMSO-d_6) δ 164.3, 157.5, 156.7, 155.5, 141.9, 140.4, 131.2, 128.7, 126.9, 126.8, 121.5, 116.9; ESR (DMSO): g = 2.006, An (G) = 15.94, ΔH (G) = 3.05. LC-MS (ESI) *m/z* (rel intensity) 585.1 ($[M(Br^{81})+2H]^+$, 100), 583.1 ($[M(Br^{79})+2H]^+$, 88); HRMS (ESI) 583.1656 for $[M+2H]^+$ (calcd 583.1663 for $C_{27}H_{32}N_6O_4Br$). HPLC purity 96.7% (MeOH: H_2O (0.1%TFA) = 56:44, 0.8 mL/min, t_R = 16.72 min).

*4.1.3.4. 4-((4-((4-((2,2,6,6-Tetramethyl-1-oxyl)carbamoyl)phenyl)amino)-5-nitropyrimidin-2-yl)amino)benzoic acid (**8d**).* Yield: 53%; Yellow solid; m.p.: 196–198℃; IR (KBr, cm^{-1}) 3234, 2970, 2616, 1723, 1656, 1604, 1531, 1440, 1329, 1175, 851, 771; ^{1}H NMR (600 MHz, DMSO-d_6) (*note compound is a free-radical, some signals appear broadened and other signals are missing) δ 9.42 (s, 1H), 8.11 (s, 2H), 8.04 (s, 2H), 7.83 (s, 2H), 7.63 (s, 2H); ^{13}C NMR (150 MHz, DMSO-d_6) δ 157.8, 153.8, 139.1, 132.4, 132.1, 131.9, 127.8, 126.4, 125.8, 124.2, 116.2, 115.1; ESR (DMSO): g = 2.006, An (G) = 15.98, ΔH (G) = 2.79. LC-MS (ESI) *m/z* (rel intensity) 550.4 ($[M+2H]^+$, 100); HRMS (ESI) 550.2407 for $[M+2H]^+$ (calcd 550.2409 for $C_{27}H_{32}N_7O_6$). HPLC purity 98.4% (MeOH: H_2O (0.1% TFA) = 68:32, 0.8 mL/min, t_R = 28.56 min).

*4.1.3.5. 4-((4-((2-Chlorophenyl)amino)-5-fluoropyrimidin-2-yl)amino)-N-(2,2,6,6-tetramethyl-1-oxyl)benzamide (**9a**)* Yield: 57%; White solid; m.p.: 137–139℃; IR (KBr, cm^{-1}) 3384, 3277, 2980, 2942, 2628, 2496, 1678, 1606, 1574, 1511, 1494, 1444, 1399,1327, 1190, 1038, 850, 776; ^{1}H NMR (600 MHz, DMSO-d_6) (*note compound is a free-radical, some signals appear broadened and other signals are missing) δ 9.46 (s, 1H), 9.33 (s, 1H), 8.18 (s, 1H), 7.64 (s, 3H), 7.60 (s, 3H), 7.48 (s, 1H), 7.41 (s, 1H); ^{13}C NMR

(150 MHz, DMSO-d_6) δ 165.0, 154.6, 150.2, 143.1, 141.1, 140.7, 139.4, 134.8, 130.0, 129.4, 128.7, 127.3, 127.1, 116.3; ESR (DMSO): g = 2.006, An (G) = 15.92, ΔH (G) = 2.85. LC-MS (ESI) *m/z* (rel intensity) 512.2 ($[M+H]^+$, 100); HRMS (ESI) 512.2090 for $[M+H]^+$ (calcd 512.2097 for $C_{26}H_{31}N_6O_2FCl$). HPLC purity 95.8% (MeOH: H_2O (0.1%TFA) = 50:50, 0.8 mL/min, t_R = 34.94 min).

*4.1.3.6. 4-((5-Chloro-4-((2-chlorophenyl)amino)pyrimidin-2-yl)amino)-N-(2,2,6,6-tetramethyl-1-oxyl)benzamide (**9b**)* Yield: 50%; White solid; m.p.: 156–158℃; IR (KBr, cm^{-1}) 3381, 3273, 2980, 2606, 2501, 1678, 1611, 1569, 1501, 1447, 1329, 1187, 1033, 853, 776, 751; ^{1}H NMR (600 MHz, DMSO-d_6) (*note compound is a free-radical, some signals appear broadened and other signals are missing) δ 9.58 (s, 1H), 8.95 (s, 1H), 8.20 (s, 1H), 7.67 (s, 1H), 7.64 (s, 1H), 7.49 (s, 5H); ^{13}C NMR (150 MHz, DMSO-d_6) δ 166.6, 165.2, 157.1, 156.4, 154.5, 142.8, 135.4, 131.4, 130.1, 129.4, 128.8, 127.5, 127.3, 117.0, 103.9; ESR (DMSO): g = 2.006, An (G) = 15.90, ΔH (G) = 2.65. LC-MS (ESI) *m/z* (rel intensity) 513.2 ($[M–O+2H]^+$, 100); HRMS (ESI) 513.1928 for $[M–O+2H]^+$ (calcd 513.1936 for $C_{26}H_{29}N_6OCl$). HPLC purity >99.9% (MeOH: H_2O (0.1%TFA) = 50:50, 0.8 mL/min, t_R = 32.93 min).

*4.1.3.7. 4-((5-Bromo-4-((2-chlorophenyl)amino)pyrimidin-2-yl)amino)-N-(2,2,6,6-tetramethyl-1-oxyl)benzamide (**9c**)* Yield: 65%; White solid; m.p.: 167–168℃; IR (KBr, cm^{-1}) 3366, 2982, 2940, 2499, 1609, 1569, 1509, 1494, 1444, 1387, 1324, 1187, 1033, 851, 768; ^{1}H NMR (600 MHz, DMSO-d_6) (*note compound is a free-radical, some signals appear broadened and other signals are missing) δ 9.60 (s, 1H), 8.70 (s, 1H), 8.28 (s, 1H), 7.74 (s, 2H), 7.63 (s, 2H) ,7.52 (s, 2H), 7.46 (s, 1H), 7.39 (s, 1H); ^{13}C NMR (150 MHz, DMSO-d_6) δ 165.1, 157.4, 157.2, 156.8, 142.6, 135.4, 129.3, 128.2, 127.4, 127.2,

126.9, 116.9; ESR (DMSO): g = 2.006, An (G) = 15.96, ΔH (G) = 2.95. LC-MS (ESI) *m/z* (rel intensity) 559.2 ([M(Br^{81})–O+2H]$^+$, 100), 557.2([M(Br^{79})–O+2H]$^+$, 80); HRMS (ESI) 557.1422 for [M–O+2H]$^+$ (calcd 557.1431 for $C_{26}H_{29}N_6OClBr$). HPLC purity 99.3% (MeOH: H_2O (0.1%TFA) = 65:35, 0.8 mL/min, t_R = 11.36 min).

*4.1.3.8. 4-((4-((2-Chlorophenyl)amino)-5-nitropyrimidin-2-yl)amino)-N-(2,2,6,6-tetramethyl-1-oxyl)benzamide (**9d**)* Yield: 71%; Yellow solid; m.p.: 208–210℃; IR (KBr, cm^{-1}) 3362, 3015, 1629, 1536, 1506, 1422, 1332, 1195,1025, 836, 726; ^{1}H NMR (600 MHz, DMSO-d_6) (*note compound is a free-radical, some signals appear broadened and other signals are missing) δ 10.66 (s, 1 H), 10.53 (s, 1 H), 9.14 (s, 1 H), 7.80–7.40 (m, 8 H); ^{13}C NMR (150 MHz, DMSO-d_6) 164.6, 158.5, 157.3, 154.1, 140.5 (2C), 134.1, 131.0, 129.4, 129.0, 127.4 (2C), 127.1 (2C), 120.5, 118.5. ESR (DMSO): g = 2.006, An (G) = 15.96, ΔH (G) = 2.95. LC-MS (ESI) *m/z* (rel intensity) 540.4 ([M+2H]$^+$, 100); HRMS (ESI) 540.2111 for [M+2H]$^+$ (calcd 540.2121 for $C_{26}H_{31}N_7O_4Cl$). HPLC purity 95.0% (MeOH:H_2O (0.1% TFA) = 65:35, 0.8 mL/min, t_R = 21.23 min).

*4.1.3.9. 4-((4-((3-Chlorophenyl)amino)-5-nitropyrimidin-2-yl)amino)-N-(2,2,6,6-tetramethyl-1-oxyl)benzamide (**9e**)* Yield: 68%; Yellow solid; m.p.: 217–219℃; IR (KBr, cm^{-1}) 3376, 3281, 3022, 1636, 1610, 1584, 1541, 1526, 1481,1414, 1329, 1202, 1137, 858, 726; ^{1}H NMR (600 MHz, DMSO-d_6) (*note compound is a free-radical, some signals appear broadened and other signals are missing) δ 10.65 (s, 1H), 10.40 (s, 1H), 9.13 (s, 1H), 7.59 (s, 5H), 7.50 (s, 3H); ^{13}C NMR (150 MHz, DMSO-d_6) δ 164.6, 158.6, 157.3, 153.9, 140.5 (2C), 135.5 (2C), 131.1, 129.4, 128.2 (2C), 127.2 (2C), 120.6, 118.8. ESR (DMSO): g = 2.006, An (G) = 15.92, ΔH (G)= 2.75.

LC-MS (ESI) *m/z* (rel intensity) 540.2 ($[M+2H]^+$, 100); HRMS (ESI) 540.2117 for $[M+2H]^+$ (calcd 540.2121 for $C_{26}H_{31}N_7O_4Cl$). HPLC purity 98.0% (MeOH: H_2O (0.1%TFA) = 72:28, 0.8 mL/min, t_R = 13.70 min).

*4.1.3.10. 4-((4-((4-Chlorophenyl)amino)-5-nitropyrimidin-2-yl)amino)-N-(2,2,6,6 tetramethyl-1-oxyl)benzamide (**9f**)* Yield: 62%; Yellow solid; m.p.: 225–227℃; IR (KBr, cm^{-1}) 3379, 2995, 1639, 1616, 1579, 1529, 1489, 1404, 1202, 841, 719; ^1H NMR (600 MHz, DMSO-d_6) (*note compound is a free-radical, some signals appear broadened and other signals are missing) δ 10.65 (s, 1H), 10.42 (s, 1H), 9.14 (s, 1H), 7.75 (s, 2H), 7.65 (s, 2H), 7.48 (s, 2H), 7.39 (s, 2H); ^{13}C NMR (150 MHz, DMSO-d_6) δ 164.5, 158.5, 157.3, 153.7, 140.4, 137.8, 132.3 (2C), 131.0, 129.7, 127.2 (2C), 125.2, 123.6, 120.6, 118.7; ESR (DMSO): g = 2.006, An (G) = 15.88, ΔH (G) = 2.85. LC-MS (ESI) *m/z* (rel intensity) 540.2 ($[M+2H]^+$, 100); HRMS (ESI) 540.2117 for $[M+2H]^+$ (calcd 540.2121 for $C_{26}H_{31}N_7O_4Cl$). HPLC purity 96.5% (MeOH: H_2O (0.1%TFA) = 72:28, 0.8 mL/min, t_R = 14.18 min).

*4.1.3.11. N-(2,2,6,6-Tetramethyl-1-oxyl)-4-((4-((2-hydroxyphenyl)amino)-5-nitropyrimidin-2-yl)amino)benzamide (**9g**)* Yield: 78%; Yellow solid; m.p.: 126–128℃; IR (KBr, cm^{-1}) 3369, 2940, 1641, 1624, 1576, 1411, 1459, 1327, 1205, 838, 746; ^1H NMR (600 MHz, DMSO-d_6) (*note compound is a free-radical, some signals appear broadened and other signals are missing) δ 10.64 (s, 1H), 10.56 (s, 1H), 10.15 (s, 1H), 9.15 (s, 1H), 7.74 (s, 4H), 7.12 (s, 1H), 6.99 (s, 2H), 6.88 (s, 1H); ^{13}C NMR (150 MHz, DMSO-d_6) δ 169.6, 165.1, 159.3, 157.7, 153.7, 141.1, 132.2, 127.6 (2C), 124.8, 121.2, 119.7 (2C), 118.8, 115.1; ESR (DMSO): g = 2.006, An (G) = 15.96, ΔH (G) = 2.95. LC-MS (ESI) *m/z* (rel intensity) 522.3 ($[M+2H]^+$, 100); HRMS (ESI) 522.2463 for

$[M+2H]^+$ (calcd 522.2459 for $C_{26}H_{32}N_7O_5$). HPLC purity 95.6% (MeOH: H_2O (0.1%TFA) = 80:20, 0.8 mL/min, t_R = 7.18 min).

*4.1.3.12. N-(2,2,6,6-Tetramethyl-1-oxyl)-4-((4-((3-hydroxyphenyl)amino)-5-nitropyrimidin-2-yl)amino)benzamide (**9h**)* Yield: 52%; Yellow solid; m.p.: 97–99℃; IR (KBr, cm^{-1}) 3324, 2985, 1678, 1619, 1591, 1529, 1422, 1332, 1207, 853, 786, 724; ^1H NMR (600 MHz, DMSO-d_6) (*note compound is a free-radical, some signals appear broadened and other signals are missing) δ 10.60 (s, 1H), 10.27 (s, 1H), 9.63 (s, 1H), 9.11 (s, 1H), 7.72 (s, 4H), 7.26 (s, 1H), 6.96 (s, 2H), 6.77 (s, 1H); ^{13}C NMR (150 MHz, DMSO-d_6) δ 167.0, 165.2, 158.9 (2C), 157.6, 154.2, 141.1, 137.7, 131.5, 129.2, 127.6 (2C), 121.5, 118.8, 116.0, 112.9; ESR (DMSO): g = 2.006, An (G) = 15.86, ΔH (G) = 2.98. LC-MS (ESI) *m/z* (rel intensity) 522.3 ($[M+2H]^+$, 100); HRMS (ESI) 522.2453 for $[M+2H]^+$ (calcd 522.2459 for $C_{26}H_{32}N_7O_5$). HPLC purity 99.8% (MeOH: H_2O (0.1%TFA) = 77:23, 0.8 mL/min, t_R = 8.14 min).

*4.1.3.13. N-(2,2,6,6-Tetramethyl-1-oxyl)-4-((4-((4-hydroxyphenyl)amino)-5-nitropyrimidin-2-yl)amino)benzamide (**9i**)* Yield: 60%; Yellow solid; m.p.: 234–236℃; IR (KBr, cm^{-1}) 3421, 3281, 2344, 1686, 1616, 1579, 1499, 1394, 1267, 1200, 841, 744, 699; ^1H NMR (600 MHz, DMSO-d_6) (*note compound is a free-radical, some signals appear broadened and other signals are missing) δ 10.56 (s, 1H), 10.21 (s, 1H), 9.61 (s, 1H), 9.09 (s, 1H), 7.67 (s, 4H), 7.32 (s, 2H), 6.86 (s, 2H); ^{13}C NMR (150 MHz, DMSO-d_6) δ 164.9, 158.7, 157.3, 155.2, 154.3, 131.0, 140.9 (2C), 127.6 (2C), 126.9 (2C), 120.4, 118.5, 114.8 (2C); ESR (DMSO): g = 2.006, An (G) = 15.94, ΔH (G) = 3.05. LC-MS (ESI) *m/z* (rel intensity) 522.4 ($[M+2H]^+$, 100); HRMS (ESI) 522.2454 for $[M+2H]^+$ (calcd 522.2459 for $C_{26}H_{32}N_7O_5$). HPLC purity 98.5% (MeOH: H_2O (0.1%TFA) = 68:32,

0.6 mL/min, t_R = 8.68 min).

*4.1.3.14. N-(2-chlorophenyl)-4-((5-fluoro-2-((4-((2,2,6,6-tetramethyl-1-oxyl) carbamoyl)phenyl)amino)pyrimidin-4-yl)amino)benzamide (**10a**)* Yield: 62%; White solid; m.p.: 213–215℃; IR (KBr, cm^{-1}) 3424, 2962, 2925, 2850, 1614, 1594, 1509, 1424, 1322, 1232, 1182, 848, 759; ^{1}H NMR (600 MHz, DMSO-d_6) (*note compound is a free-radical, some signals appear broadened and other signals are missing) δ 9.92 (s, 1H), 9.74 (s, 1H), 9.62 (s, 1H), 8.24 (s, 1H), 8.02 (s, 4H), 7.80 (s, 4H), 7.66 (s, 1H), 7.55 (s, 1H), 7.39 (s, 1H), 7.28 (s, 1H); ^{13}C NMR (150 MHz, DMSO-d_6) δ 165.4, 164.5, 154.7, 149.1, 143.2, 142.1, 141.5, 141.1, 139.8, 134.9, 129.5, 128.9, 128.1, 127.6, 127.5, 127.0, 119.8, 117.1. ESR (DMSO): g = 2.006, An (G) = 15.96, ΔH (G) = 2.97. LC-MS (ESI) *m/z* (rel intensity) 632.3 ($[M+2H]^+$, 100); HRMS (ESI) 632.2542 for $[M+2H]^+$ (calcd 632.2547 for $C_{33}H_{36}N_7O_3FCl$). HPLC purity 95.6% (MeOH: H_2O (0.1%TFA) = 60:40, 0.8 mL/min, t_R = 21.46 min).

*4.1.3.15. N-(2-chlorophenyl)-4-((2-((4-((2,2,6,6-tetramethyl-1-oxyl)carbamoyl)phenyl) amino)-5-nitropyrimidin-4-yl)amino)benzamide (**10b**)* Yield: 79%; Yellow solid; m.p.: 274–276℃; IR (KBr, cm^{-1}) 3404, 2995, 1656, 1631, 1539, 1424, 1332, 1222, 853, 766; ^{1}H NMR (600 MHz, DMSO-d_6) (*note compound is a free-radical, some signals appear broadened and other signals are missing) δ 10.67 (s, 1H), 10.52 (s, 1H), 10.08 (s, 1H), 9.15 (s, 1H), 8.06 (s, 3H), 7.98–7.29 (m, 9H); ^{13}C NMR (150 MHz, DMSO-d_6) δ 164.7, 164.1, 158.7, 157.5, 153.8, 140.5, 139.8, 134.6, 131.4, 129.8, 129.0, 127.8 (4C), 127.2 (2C), 124.4, 121.2, 119.2; ESR (DMSO): g = 2.006, An (G) = 15.96, ΔH (G) = 2.92. LC-MS (ESI) *m/z* (rel intensity) 659.2 ($[M+2H]^+$), 643.3 ($[M–O+2H]^+$, 100); HRMS (ESI) 659.2490 for $[M+2H]^+$ (calcd 659.2492 for $C_{33}H_{36}N_8O_5Cl$). HPLC purity 99.7% (MeOH:

H_2O (0.1%TFA) = 75:25, 0.8 mL/min, t_R = 9.47 min).

*4.1.3.16. N-(3-chlorophenyl)-4-((2-((4-((2,2,6,6-tetramethyl-1-oxyl)carbamoyl) phenyl)amino)-5-nitropyrimidin-4-yl)amino)benzamide (**10c**)* Yield: 92%; Yellow solid; m.p.: 248–249°C; IR (KBr, cm^{-1}) 3394, 2980, 2364, 1668, 1624, 1531, 1427, 1334, 1220, 851, 761; ^{1}H NMR (600 MHz, DMSO-d_6) (*note compound is a free-radical, some signals appear broadened and other signals are missing) δ 10.66 (s, 1H), 10.50 (s, 1H), 10.39 (s, 1H), 9.14 (s, 1H), 8.03 (s, 4H), 7.93–7.37 (m, 7H), 7.15 (s, 1H); ^{13}C NMR (150 MHz, DMSO-d_6) δ 165.0, 164.7 (2C), 159.1, 157.7, 153.9, 140.8, 140.5, 140.1, 132.9, 131.7, 130.7, 128.1 (3C), 127.5 (2C), 124.2, 123.5, 121.3, 119.7, 119.6 (2C). ESR (DMSO): g = 2.006, An (G) = 15.92, ΔH (G) = 2.90. LC-MS (ESI) *m/z* (rel intensity) 659.2 ($[M+2H]^+$, 100), 643.3 ($[M–O+2H]^+$); HRMS (ESI) 659.2507 for $[M+2H]^+$ (calcd 659.2492 for $C_{33}H_{36}N_8O_5Cl$). HPLC purity 98.7% (MeOH: H_2O (0.1%TFA) = 75:25, 0.8 mL/min, t_R = 7.96 min).

*4.1.3.17. N-(4-chlorophenyl)-4-((2-((4-((2,2,6,6-tetramethyl-1-oxyl)carbamoyl) phenyl) amino)-5-nitropyrimidin-4-yl)amino)benzamide (**10d**)* Yield: 93%; Yellow solid; m.p.: 275–277°C; IR (KBr, cm^{-1}) 3401, 2980, 2379, 1609, 1536, 1504, 1414, 1329, 1210, 853, 788; ^{1}H NMR (600 MHz, DMSO-d_6) (*note compound is a free-radical, some signals appear broadened and other signals are missing) δ 10.70 (s, 1H), 10.53 (s, 1H), 10.40 (s, 1H), 9.16 (s, 1H), 8.05 (s, 3H), 7.84–7.58 (m, 7H), 7.42 (brs, 2H); ^{13}C NMR (150 MHz, DMSO-d_6) δ 165.1, 164.6 (2C), 159.1, 157.8, 154.1, 140.9, 140.1, 138.3, 131.1, 129.1, 128.1 (4C), 127.6 (2C), 127.3, 124.5, 123.4, 121.1, 119.5. ESR (DMSO): g = 2.006, An (G) = 15.94, ΔH (G) = 2.92. LC-MS (ESI) *m/z* (rel intensity) 681.2 ($[M+H+Na]^+$, 100), 659.2 ($[M+2H]^+$), 643.3 ($[M–O+2H]^+$); HRMS (ESI) 659.2495 for $[M+2H]^+$ (calcd

659.2492 for $C_{33}H_{36}N_8O_5Cl$). HPLC purity 97.7% (MeOH: H_2O (0.1%TFA) = 75:25, 0.8 mL/min, t_R = 9.80 min).

4.1.3.18. N-(2-chlorophenyl)-4-((5-fluoro-2-((4-((1-methylpiperidin-4-yl)carbamoyl) phenyl)amino)pyrimidin-4-yl)amino)benzamide ***(11)*** Yield: 42%; White solid; m.p.: 246–248℃; IR (KBr, cm^{-1}) 3385, 2965, 1683, 1618, 1519, 1440, 1379, 800, 722; ^1H NMR (600 MHz, DMSO-d_6) δ 10.92 (s, 1H), 10.05 (s, 1H), 10.03 (s, 1H), 9.96 (s, 1H), 8.44 (d, J = 7.2 Hz, 1H), 8.42–8.28 (m, 1H), 8.04–7.95 (m, 3H), 7.85–7.80 (m, 2H), 7.73–7.68 (m, 2H), 7.62–7.53 (m, 1H), 7.38–7.35 (m, 1H), 7.29–7.27 (m, 1H), 3.78 (s, 1H), 3.40–3.34 (m, 1H), 2.66 (s, 3H), 1.99–1.97 (m, 4H), 1.37–1.26 (m, 4H); ^{13}C NMR (150 MHz, DMSO-d_6) δ 165.4, 164.7, 153.9, 150.0, 143.5, 141.7, 141.6, 140.0, 135.3, 135.2, 129.4 (2C), 128.6, 128.4 (3C), 128.1 (2C), 127.4, 127.3, 127.2, 127.0, 120.6, 117.7, 52.5 (2C), 44.3, 42.4, 28.7 (2C); MS (ESI) *m/z* (rel intensity) 574.2 ($[M+H]^+$, 100). HPLC purity 95.2% (MeOH: H_2O (0.1%TFA) = 70:30, 0.8 mL/min, t_R = 12.81 min).

4.2. Biology

4.2.1 Antiproliferation assays

Cells were incubated at 37 ℃ in a 5% CO_2 atmosphere, and were plated in 96-well plates and allowed to attach for 4–6 h, the synthetic compounds and reference compound VX-680 were dissolved in DMSO as initial concentration and then exposed to different concentrations of the test compounds for 48 h. Following 5 mg/mL MTT were added to each well for another 4 h, then the solution was centrifuged for 10 min under 2000 rpm. The supernatant was mixed with 150 μL DMSO, and shaken on an oscillator. The absorbance at λ_{490} was determined on a plate reader. IC_{50} values were determined from a

log plot of percent of control versus concentration.

4.2.2 Aurora inhibition

The synthetic compounds and VX-680 were dissolved and diluted to five concentrations (0.1, 1, 10, 100 and 1000 nM) in the PBS, and added 5 μL above solution to the 50 μL reaction mixture (40 mM Tris-HCl (pH 7.4), 10 mM $MgCl_2$, 1 mM DTT, 0.1 mg/mL BSA, 10 μM ATP, 0.2 μg/mL Kinase and 100 μM Kemptide acetate salt), then the kinase reactions were incubated for 30 min at 37 °C. The assay was performed using Kinase-Glo Plus luminescence kinase assay kit. The IC_{50} values were calculated using nonlinear regression with normalized dose-response fit using Prism Graph Pad software.

4.2.3 Western blot analysis

HeLa cells were lysed with mammalian lysis buffer or containing phosphatase and protease inhibitors. For total cell protein extracts, cells were washed and lysed in lysis buffer (50 mM Tris-HCl (pH 7.5), 1% NP-40, 2 mM EDTA, 10 mM NaCl, 10 μg/ml Aprotinin, 10 μg/ml Leupeptin, 1 mM DTT, 0.1% SDS and 1 mM phenyl methyl sulfonyl fluoride). Total proteins were achieved by centrifuging (12,000 g for 20 min at 4℃). Protein content of cell lysates was measured with the BCA protein assay reagent (Beyotime, Jiangsu, China), and samples containing equal amounts of protein were used for analysis. Lysates were boiled in sample buffer containing β-mercaptoethanol for 5 min. Proteins were then subjected to 10% SDS-PAGE and transferred to polyvinylidine difluoride (PVDF) membranes (Millipore Corporation, USA). After blocking with 5% BSA for 2 h at room temperature, and then incubated with dilute solution (1:500–1:1000) of the antibody against AurA and AurB (Abcam), the antibody against phospho-AurA

(Thr288) and phospho-AurB (Thr232) (Cell Signaling Technology), the antibodies against cyclinB1 and cdc2 (BioLegend), the antibodies against BAD, Bax, Bcl-2, caspase-3, caspase-9 and the antibody against β-actin (ZSGB-BIO) in blocking buffer overnight at 4℃. The blot was then incubated with appropriate secondary antibody (1:5000–1:10000 dilution), β-Actin was used as a loading control. The protein bands were visualized using the Gel Imaging System (ChemDoc-It610, UVP, USA).

4.2.4 ELISA experiment

HeLa human tumor cells were grown in 6-well cell culture dishes for 12 h with **10a** diluted in DMSO at various concentrations. Use purified Human Aurora A or B antibody to coat microtiter plate wells, make solid-phase antibody, then add whole cell lysate including Aurora A or B to wells, combined Aurora A or B which with HRP labeled, become antibody-antigen-enzyme-antibody complex, after washing completely, Add TMB substrate solution, TMB substrate becomes blue color at HRP enzyme-catalyzed, reaction is terminated by the addition of a sulphuric acid solution and the color change is measured spectrophotometrically at a wavelength of 450 nm.

4.2.5 Cell immunofluorescence microscopy

HeLa cells plated on coverslips were either untreated or treated with various concentrations of compound **10a**. After 24 h, the cells were fixed with 4% paraformaldehyde and permeabilized in 0.1% Triton X-100 and 2% bovine serum albumin as described previously. For microtubule staining, the samples were incubated with primary anti-α-tubulin mouse antibody (Cell Signaling Technology) at 4 ℃ for overnight, washed with PBS three times, then with FITC-conjugated secondary antibody

(Invitrogen, Carlsbad, CA, USA) for 2 h at room temperature. The nuclear DNA was then stained with DAPI (Molecular Probes Inc., Eugene, OR, USA). Cells were analyzed under a confocal microscope (FV-1000; Olympus, Tokyo, Japan).

4.2.6 Cell cycle profiling

HeLa human tumor cells were grown in 6-well cell culture dishes for 12 h with **10a** diluted in DMSO at various concentrations. The cells were stained with propidium iodide (Molecular Probes), and DNA cell cycle profiling was determined by measuring DNA content by using flow cytometry (FACScan, Bection Dickinson). The percentage of G1, S, G2/M cells was calculated by using ModFit LT version 3.0.

4.2.7 Apoptosis assay

HeLa cells (2×10^5 cells/ml) were plated in 6-well plates and then treated with vehical, 0.1 μM, 1 μM and 5 μM of **10a**. The cells were incubated at 37 ℃, 5% CO_2 for 12 h. Then the cells were collected by centrifugation at 1000 r/min and washed twice with ice-cold PBS. Afterwards, the cells were suspended in 500 μL annexin V binding buffer and 5 μL each of annexin V and PI were added to these samples. Next, these samples were incubated for 30 min at room temperature and then assayed by flow cytometric analysis (FACScan, Bection Dickinson).

4.2.8 Molecular docking study

The docking simulation was performed using the Glide module of Schrödinger. Before docking, the protein structure and ligand **10a** were minimized firstly by Schrödinger. The crystal waters were removed and the Kollman united atom charges and

polar hydrogen was added to the two proteins. The ligand in the crystal structure was used to determine the location of a docking grid box and was then removed prior to grid generation in next step. Gasteiger charges were assigned to the new constructed structures in Schrödinger. At the same time, the Non-polar hydrogen atoms were merged and the rotatable bonds were defined. Based on the ligand in the crystal structure, the grid maps of the protein were produced using Grid module embedded in Schrödinger software. As result, a grid size of 60×60×66 Å points and 0.375 Å spacing were generated. Each docking process was performed in 250000 energy evaluation with 10 conformations kept and the most favorable pose of each compound was displayed.

Acknowledgments

This work was supported by the National Natural Sciences Foundations of China (Nos. 21372110 and 21672093).

References

[1] Vader G, ALens SM. The Aurora kinase family in cell division and cancer. *Bioch. Biophy. Acta*. 2008; 1786: 60–72.

[2] Fu J, Bian M, Jiang Q, Zhang C. Roles of aurora kinases in mitosis and tumorigenesis. *Mol. Cancer. Res*. 2007; 5: 1–10.

[3] Carmena M, Earnshaw WC. The cellular geography of Aurora kinases. *Nat. Rev. Mol. Cell. Biol*. 2003; 4: 842–854.

[4] Marumo T, Zhang D, Saya, H, Aurora-A: a guardian of poles, *Nat. Rev. Cancer*. 2005; 5: 42−50.

[5] Yan M, Wang C, He B, et al. Aurora-A kinase: A potent oncogene and target for cancer therapy, *Med. Res. Rev*. 2016; 36: 1036–1079.

[6] Vader G, Medema RH, Lens SM. The chromosomal passenger complex: guiding Aurora-B through mitosis, *J. Cell. Biol*. 2006; 173: 833−837.

[7] Sasai K, Katayama H, Stenoien DL, et al. Aurora-C kinase is a novel chromosomal passenger protein that can complement Aurora-B kinase function in mitotic cells, *Cell Motil. Cytoskelet*. 2004; 59: 249−263.

[8] Pollard JR, Mortimore M, Discovery and development of Aurora kinase inhibitors as anticancer agents, *J. Med. Chem*. 2009; 52: 2629−2651.

[9] Katayama H, Sen S, Aurora kinase inhibitors as anticancer molecules, *Biochim. Biophys. Acta*. 2010; 1799: 829−839.

[10] Borisa AC, Bhatt HG, A comprehensive review on Aurora kinase: Small molecule inhibitors and clinical trial studies, *Eur. J. Med. Chem*. 2017; 140: 1−19.

[11] Tyler RK, Shpiro N, Marquez R. VX-680 inhibits Aurora A and Aurora B kinase

activity in human cells, *Cell Cycle.* 2007; 6: 2846−2854.

[12]Harrington EA, Bebbington D, Moore J. VX-680, a potent and selective small-molecule inhibitor of the aurora kinases, suppresses tumor growth in vivo, *Nat. Med.* 2004; 10: 262−267.

[13]Manfredi MG, Ecsedy JA, Meetze KA, et al. Antitumor activity of MLN8054, an orally active small-molecule inhibitor of aurora A kinase, *Proc. Natl. Acad. Sci. USA*. 2007; 104: 4106−4111.

[14]Zhang S, Farag SS. From cell biology to therapy, ENMD-2076 in the treatment of multiple myeloma, *Expert Opin. Investig. Drugs.* 2011; 20: 1015–1028.

[15]Geunsmeyer S, Cee VJ, Deak HL, et al. Discovery of *N*-(4-(3-(2-Aminopyrimidin-4-yl)pyridin-2-yloxy) phenyl)-4-(4-methylthiophen- 2-yl) phthalazin-1-amine (AMG 900), A highly selective, orally bioavailable inhibitor of Aurora kinases with activity against multidrug-resistant cancer cell lines, *J. Med. Chem.* 2015; 58: 5189–5207.

[16]Wang S, Midgley CA, Scaërou F, et al. Discovery of *N*-phenyl-4-(thiazol-5-yl) pyrimidin-2-amine aurora kinase inhibitors. *J. Med. Chem.* 2010; 53: 4367–4378.

[17]Jani JP, Arcari J, Bernardo V, et al. PF-03814735, an orally bioavailable small molecule aurora kinase inhibitor for cancer therapy, *Mol. Cancer. Ther.* 2010; 9: 883−894.

[18]Hook KE, Garza SJ, Lira ME, et al. An integrated genomic approach to identify predictive biomarkers of response to the aurora kinase inhibitor PF-03814735, *Mol. Cancer Ther.* 2012; 11: 710−719.

[19]Likhtenshtein GI, Yamauchi J, Nakatsuji SI, Nitroxides: applications in chemistry,

biomedicine, and materials science, *John Wiley & Sons,* 2008.

[20]Gariboldi MB, Ravizza R, Petterino C, et al. Study of in vitro and in vivo effects of the piperidine nitroxide Tempol–a potential new therapeutic agent for gliomas, *Eur. J. Cancer.* 2003; 39: 829–837.

[21]Matsumoto KI, Hyodo F, Matsumoto A, et al. High-resolution mapping of tumor redox status by magnetic resonance imaging using nitroxides as redox-sensitive contrast agents, *Clin. Cancer Res.* 2006; 12: 2455–2462.

[22]Borbat PP, Costafilho AJ, Earle KA, et al. Freed, Electron spin resonance in studies of membranes and proteins, *Science.* 2001; 291: 266–269.

[23]Vazquez J, Tautz L, Ryan JJ, et al. Development of molecular probes for second-site screening and design of protein tyrosine phosphatase inhibitors, *J. Med. Chem.* 2007; 50: 2137–2143.

[24]Cecchi A, Ciani L, Winum JY, et al. Carbonic anhydrase inhibitors: Design of spin-labeled sulfonamides incorporating TEMPO moieties as probes for cytosolic or transmembrane isozymes, *Bioorg. Med. Chem. Lett.* 2008; 18: 3475–3480.

[25]Li S, Guo C, Sun X, et al. Synthesis and biological evaluation of quinazoline and quinoline bearing 2,2,6,6-tetramethylpiperidine-*N*-oxyl as potential epidermal growth factor receptor (EGFR) tyrosine kinase inhibitors and EPR bio-probe agents, *Eur. J. Med. Chem.* 2012; 49: 271–278.

[26]Jin Y, Chen SW, X Tian, Synthesis and biological evaluation of new spin-labeled derivatives of podophyllotoxin, *Bioorg. Med. Chem.* 2006; 14: 3062–3068.

[27]Zhang ZW, Zhang JQ, Hui L, et al. First synthesis and biological evaluation of novel spin-labeled derivatives of deoxypodophyllotoxin. *Eur. J. Med. Chem.* 2010; 45: 1673–1677.

[28]Aliagas-Martin I, Burdick D, Corson L, et al. A class of 2,4-bisanilinopyrimidine Aurora A inhibitors with unusually high selectivity against Aurora B, *J. Med. Chem.* 2009; 52: 3300–3307.

[29]Lawrence HR, Martin MP, Luo Y, et al. Development of *o*-chlorophenyl substituted pyrimidines as exceptionally potent aurora kinase inhibitors, *J. Med. Chem.* 2012; 55: 7392–7416.

[30]Liu M, Wang S. Clampit JE, et al. Discovery of a new class of 4-anilinopyrimidines as potent c-Jun *N*-terminal kinase inhibitors: synthesis and SAR studies, *Bioorg. Med. Chem. Lett.* 2007; 17: 668−672.

[31]Lietha D, Eck MJ, Crystal structures of the FAK kinase in complex with TAE226 and related bis-anilinopyrimidine inhibitors reveal a helical DFG conformation, *PLoS One.* 2008; 3: e3800.

[32]Bardelle C, Cross D, Davenport S,et al. Inhibitors of the tyrosine kinase EphB4. Part 1: Structure-based design and optimization of a series of 2,4-bis-anilinopyrimidines, *Bioorg. Med. Chem. Lett.* 2008; 18: 2776−2780.

[33]Bardelle C, Coleman T, Cross D, et al. Inhibitors of the tyrosine kinase EphB4. Part 2: Structure based discovery and optimisation of 3,5-bis substituted anilinopyrimidines, *Bioorg. Med. Chem. Lett.* 2008; 18: 5717−5721.

[34]Breslin HJ, Lane BM, Ott GR, et al. Dorsey. Design, synthesis, and anaplastic lymphoma kinase (ALK) inhibitory activity for a novel series of

2,4,8,22-tetraazatetracyclo[14.3.1.1^{3,7}.1^{9},^{13}]docosa-1(20),3(22),4,6,9(21),10,12,16,18- nonaene macrocycles, *J. Med. Chem.* 2012; 55: 449−464.

[35]Jang J, Son JB, To C, et al. Discovery of a potent dual ALK and EGFR T790M inhibitor, *Eur. J. Med. Chem.* 2017; 136: 497−510.

[36]Podar K, Tonon G, Sattler M, et al. The small-molecule VEGF receptor inhibitor pazopanib (GW786034B) targets both tumor and endothelial cells in multiple myeloma, *Proc Natl Acad. Sci. USA.* 2006; 103: 19478–19483.

[37]Beattie JF, Breault GA, Ellston RP, et al. Cyclin-dependent kinase 4 inhibitors as a treatment for cancer. Part 1: Identification and optimisation of substituted 4,6-bisanilinopyrimidines, *Bioorg. Med. Chem. Lett.* 2003; 13: 2955−2960.

[38]Qin WW, Sang CY, Zhang LL, et al. Synthesis and biological evaluation of 2,4-diaminepyrimides as selective Aurora A kinase inhibitors, *Eur. J. Med. Chem.* 2015; 95: 174–184.

[39]Song Z, Yang Y, Liu Z, et al. Discovery of novel 2,4-diarylaminopyrimidine analogues (DAAP alogues) showing potent inhibitory activities against both wild-type and mutant ALK kinases, *J. Med. Chem.* 2015; 58: 197−211.

[40] Long L, Luo Y, Hou ZJ, et al. Synthesis and biological evaluation of aurora kinases inhibitors based on *N*-trisubstituted pyrimidine scaffold, *Eur. J. Med. Chem.* 2018; 145: 805–812.

[41]Kashem MA, Nelson RM, Yingling JD, et al. Three mechanistically distinct kinase assays compared: measurement of intrinsic ATPase activity identified the most comprehensive set of ITK inhibitors, *J. Biomol. Screen.* 2007; 12: 70–83.

[42]Lin Z-Z, Jeng Y-M, Hu F-C, et al. Significance of Aurora B overexpression in

hepatocellular carcinoma. *BMC Cancer*. 2010; 10, 461–474.

[43]Littlepage LE, Wu H, Andresson T, et al. Identification of phosphorylated residues that affect the activity of the mitotic kinase Aurora-A, *Proc. Natl. Acad. Sci.* 2002; 99: 15440–15445.

[44]Yoshihiro Y, Takeshi U, Aie K, et al. Autophosphorylation of a newly identified site of Aurora-B is indispensable for cytokinesis, *J. Biol. Chem.* 2004;279: 12997–13003.

[45]Carpinelli P, Moll J. Aurora Kinases and Their Inhibitors: More Than One Target and One Drug, Targeted Therapies in Cancer. *Springer New York*, 2008: 54-73.

[46]Wang W, Feng X, Liu HX, et al. Synthesis and biological evaluation of 2,4-disubstituted phthalazinones as Aurora kinase inhibitors, *Bioorg. Med. Chem.* 2018; 26: 3217–3226.

[47]Nar A, Ozen O, Tutuncu NB, Demirhan B. Cyclin A and cyclin B1 overexpression in differentiated thyroid carcinoma, *Med. Oncol.* 2012; 29: 294–300.

[48]He SJ, Shu LP, Zhou ZW, et al. Inhibition of Aurora kinases induces apoptosis and autophagy via AURKB/p70S6K/RPL15 axis in human leukemia cells, *Cancer Lett.* 2016; 382: 215–230.

[49]Hailt MM, Ebrahim HY, Mohyeldin MM, et al. The tobacco cembranoid (1*S*,2*E*,4*S*,7*E*,11*E*)-2,7,11-cembratriene-4,6-diol as a novel angiogenesis inhibitory lead for the control of breast malignancies, *Bioorg. Med. Chem.* 2017; 25: 3911–3921.

[50]DeLano WL, The PyMOL Molecular Graphics System, 2002. DeLano Scientific, *Palo Alto, CA, USA.*

Synthesis and identification of 2,4-bisanilinopyrimidines bearing 2,2,6,6-tetramethylpiperidine-*N*-oxyl as potential Aurora A inhibitors

Chun-Yan Sang, Wen-Wen Qin, Xiu-Juan Zhang, Yu Xu, You-Zhen Ma, Xing-Rong Wang, Ling Hui, Shi-Wu Chen

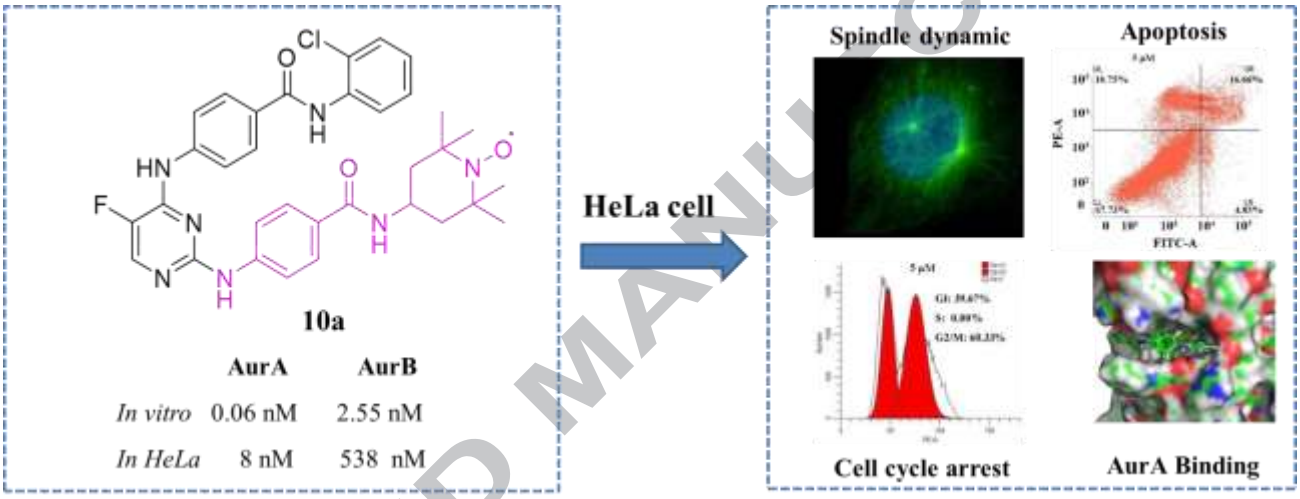

A series of stable nitroxyl radicals labeled 2,4-diaminopyrimidines exert their anti-proliferations in human tumor cell lines through targeting inhibition of Aurora A kinases.

Research highlights:

1. 2,4-Bisanilinopyrimidines bearing nitroxides display potent anti-proliferations.
2. Compound **10a** shows selectivity inhibitions for Aurora A over Aurora B.
3. Compound **10a** disrupt the spindle formation.
4. Compound **10a** blocks G2/M cell cycle arrest in HeLa cells.
5. Compound **10a** induces apoptosis in HeLa cells.